Kinetics of Peptide Aggregation

Keira C. Ebanks

Thesis submitted to the faculty of the Virginia Polytechnic Institute and State University
in partial fulfillment of the requirements for the degree of

Master of Science In
Biological Systems Engineering

Justin R. Barone
Amy J. Pruden-Bagchi
Jactone A. Ogejo

April 20, 2011
Blacksburg, VA

Keywords: peptide, cross-beta, amyloids, protein aggregation, kinetics

Kinetics of Peptide Aggregation

Keira C. Ebanks

ABSTRACT

The most thermodynamically stable biological structure is the cross-β secondary structure of the "amyloid" or "prion". As a testament to its stability, the amyloid occurs naturally in 2 rare instances: as a mechanism to protect or destroy life. Pathogenic amyloids are the signature of neurological disorders such as Alzheimer's and Parkinson's disease and bovine spongiform encephalopathy (BSE), which have no effective treatments or known cures. Pathogenic amyloids appear as nanometer sized "plaques" that self-assemble over time. The plaques usually are well-organized crystalline/fibrous structures ~10-20 nm in diameter and >100 nm long. "Functional" amyloids are very rare in nature and serve the direct purpose to proliferate life. Stalks to protect eggs, fibers to coat spores, and adhesive proteins of bacteria, algae, fungi, and mollusks are examples. Functional amyloids can be larger than pathogenic amyloids by 1-2 orders of magnitude.

There is a burgeoning research field based on emulating the amyloid. This is because it can be formed from a host of proteins or peptides simply by denaturing them enough to form a cross-β secondary structure and has a modulus of >10 GPa. As a general reference, "protein" is usually a very high molecular weight, naturally occurring molecule and "peptide" is a much smaller portion of a natural protein or a non-natural molecule synthesized from a few amino acids. Researchers are increasingly attempting to take advantage of the functional amyloid. It is still not understood how the functional amyloid self-assembles or why it can be larger than the pathogenic amyloid. We have identified a potential pathway to large functional amyloids that involves a long α-helix containing protein (the "adder") undergoing an $\alpha \rightarrow \beta$ transition in the presence of a hydrophobic β-sheet template. Testing our hypothesis against proteins found in natural large functional amyloids seems to suggest it is a ubiquitous process. The resulting material is a fiber composite similar to the native structures.

Acknowledgements

I would like to thank and acknowledge my family and friends for taking this journey with me. I would also like to thank my committee chair, Dr. Barone, for his guidance and patience, and advisement. Also, I would like to express my gratitude to my committee members, Dr. Pruden-Bagchi and Dr. Arogo for their support, cooperation, and commitment.

Table of Contents

List of Figures

List of Tables

Chapter 1: Introduction

Proteins are one of the macromolecular building blocks for all living things. In the human body, proteins serve many functions including maintaining structure and catalyzing reactions. The versatility of proteins in living organisms is achieved by primary, secondary, tertiary, and quaternary structures [1,2]. Proteins are polymers composed of various combinations of the 20 naturally occurring amino acid monomers. The primary structure is the sequence of amino acids in the polymer. Based on the various possible combinations to add amino acids into the polymer, portions of the protein can then arrange into well-defined shapes (β-sheets or α-helices) or not (random coils). This is known as the secondary structure. Based on entropy and enthalpy considerations, the amino acid sequence will determine the final shape of the protein or tertiary structure. Finally, the manner in which individual proteins interact with one another defines the quarternary structure. In many cases, individual proteins will interact with one another on the secondary structure level. For this research, the secondary structure is the most important because it is the biggest determiner of properties and in our hypothesized system has the ability to change. The different secondary structures are alpha (α) helix, beta (β) sheet and random coils [1,2]. When examining the secondary structure, stabilization of the surrounding conditions i.e., temperature and pH, are very important. In confined cell spaces, the probability of protein aggregation is much higher than in less confined space so concentration is also important. Protein aggregation is promoted by misfolded or unfolded proteins [1]. This promotion is heavily related to its primary structure, the amino acid sequence, at a given environmental condition.

The specific objective of this research is to better understand the dynamics of peptide self-assembly or aggregation. Specifically, we have identified a route to self-assemble very large peptide fibers from the molecular to the macroscopic scale, which is unusual. Some of the fibers have surface features and size similarities to many naturally occurring fibers, including silk and keratin, possibly pointing to a universal aggregation process. Examples of some large self-assembled fibers are shown in Figure 1.

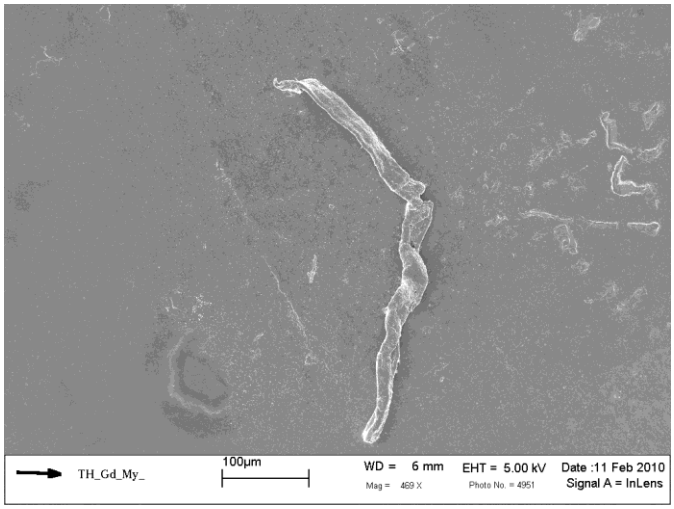

(a) Gd:My 1:3

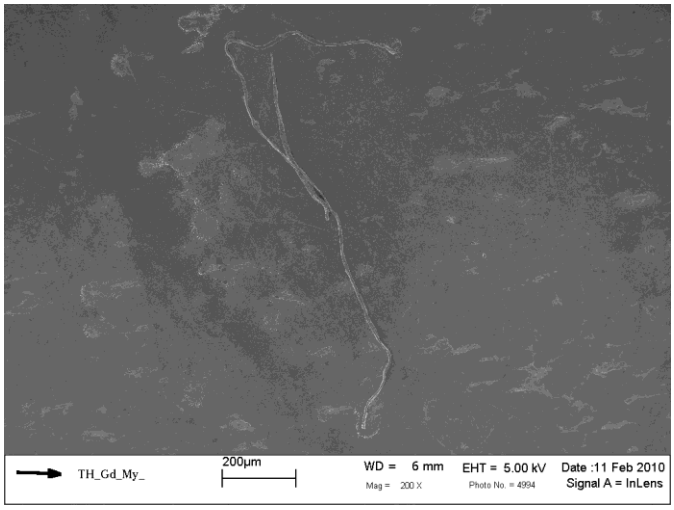

(b) Gd:My 1:1

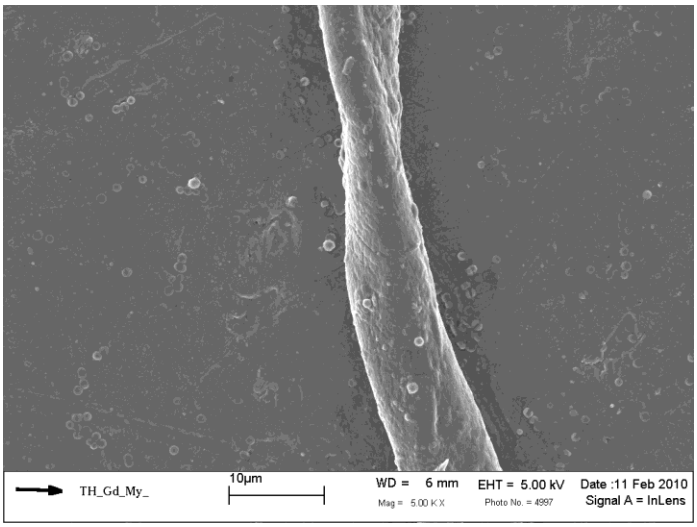

(c) Gd:My 1:1

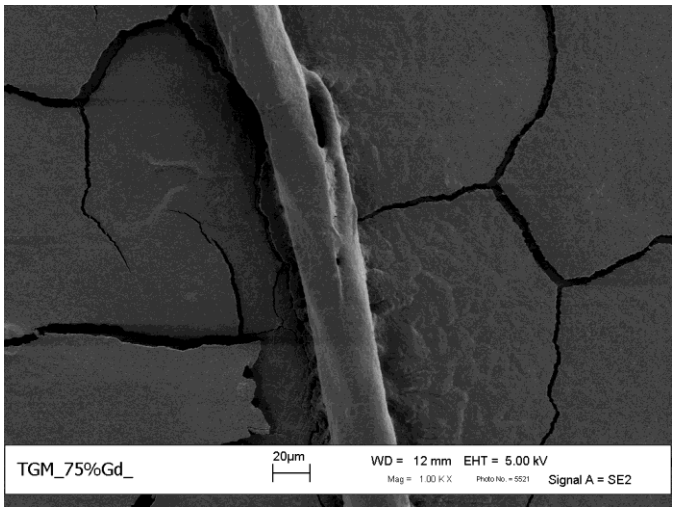

(d) Gd:My 3:1

Figure 1 Scanning electron micrographs (SEM) of large gliadin-myoglobin (Gd-My) fibers self-assembled in our laboratory.

Characterization of this fiber has thus far revealed:

1. The fiber has an elementary cross-β secondary structure, similar to amyloids or "prions" [3-4].
2. The fiber can only form from peptide mixtures [3-4].

3. Fibers can be rectangular or round in cross-section [4].

These initial observations of fiber characterization were made on tryptic hydrolysates of wheat gluten. Wheat gluten is the general term for the protein portion of wheat. Wheat gluten is actually a combination of three proteins: gliadin (Gd), low molecular weight glutenin (GtL), and high molecular weight glutenin (GtH). Tryptic hydrolysates of the individual components of wheat gluten did not produce large fibers, suggesting it was a specific combination of the tryptic peptides that caused fiber self-assembly from the nanometer to the micrometer scale. Fourier transform-infrared (FT-IR) spectroscopy and x-ray diffraction (XRD) results showed tryptic peptides of gliadin were strong cross-β formers but tryptic peptides of glutenin were not. An analysis of the structures of the tryptic peptides showed that one of the gliadin peptides, Gd20, had a strong propensity for cross-β formation [4].

Gd20 was also predominantly hydrophobic as shown in Tables 2 and 3 [34]. Further analysis showed that one of the glutenin peptides, GtL75, had a lot of α-helix, was much less hydrophobic than Gd20, and had some propensity for cross-β formation but not as much as Gd20. This led us to hypothesize that self-assembling large fibers required a short hydrophobic peptide to form a β-sheet "template" that would cause a longer α-helix peptide to undergo an α to β transition and add to the template thus building the fiber. The goal of the research was to test a part of this hypothesis by self-assembling myoglobin, a full protein that met all of the criteria of the "adder", and trypsin hydrolyzed gliadin.

1.1 Protein folding and unfolding

The native state and function of proteins is highly dependent on the amino acid sequence [5]. It is the amino acid sequence or primary structure that determines the protein's properly folded configuration. Upon unfolding, one thing that might happen to a protein is cross-β sheet formation. Protein misfolding promotes organized amyloid formation. Protein misfolding can be caused by denaturation or severe changes in the protein environment, such as changes in temperature, pH, or ionic strength [3,6]. At physiological conditions where severe environmental changes are rare, it is not well understood what causes protein misfolding except for perhaps rare genetic mutations to the protein [6,7].

1.2 Peptide Self-assembly

Protein-protein interactions play an important role in metabolic and degradation processes, in self-assembling large biological structures, and in determining the properties of biological structures [8]. Self-assembly in biology is popularized by the cross-β fibril formation, also known as amyloids [9-12]. The cross-β fiber consists of peptide chains that align perpendicular to the fibril axis, shown in Figure 2. Native β-sheet fibers like silk and keratin have the protein chains aligned parallel to the fiber axis.

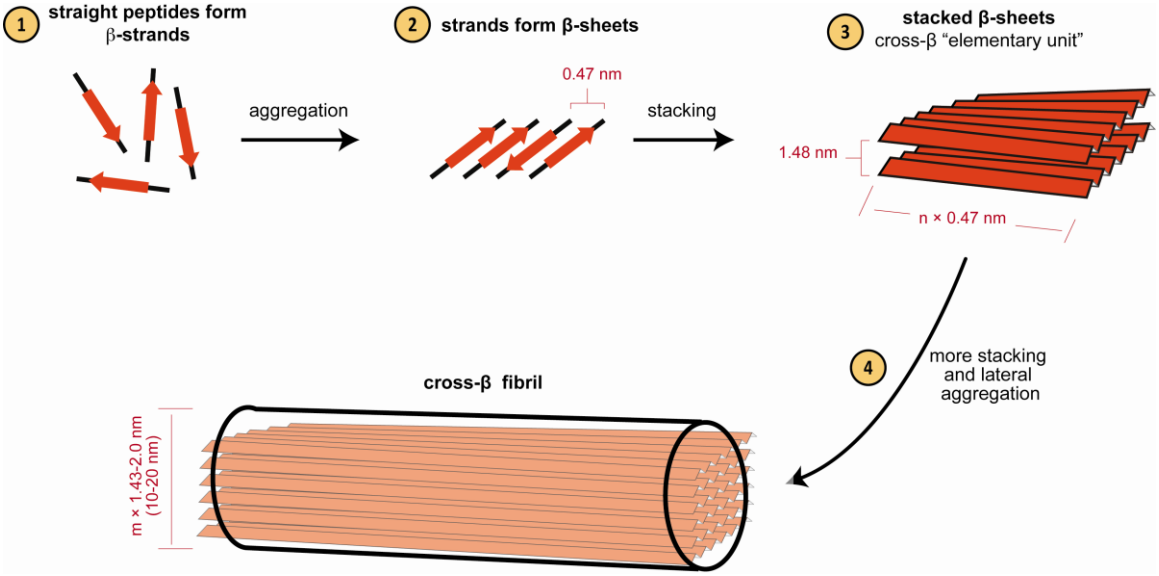

Figure 2 Cross beta structure perpendicular to fibril axis

An additional method of peptide self-assembly is done by "charge complementarity". Peptide chains possess opposite charges and pair together based on attraction [8]. Lopez de la Paz *et al*. investigated *in vitro* aggregation of β-sheet secondary structures into amyloid fibers using a molecular dynamics simulation [13]. With this method all amino acid sequences that had the potential to self-assemble into the β-sheet structure were selected and researched further. Based on an assumption regarding a direct relation of stacking of β-sheets and self-assembly of amyloid fibers, a "six stranded antiparallel β-sheet" was devised. Their hypothesis was based on the effect of net charge of the sequence and the charge effects on self-assembly. For further exploration the pH was varied between acidic and basic conditions along with net charge amendments. Sequences in the basic environments with a -1 net charge produced amyloid fiber formation through self-assembly with common morphologies. The morphologies were not specifically listed but it was stated that the β-sheet structure was predominant in all of

the tested sequences. In the case of acidic environments and a net charge of +1 the self-assembled amyloids had many uncommon morphologies [13]. These results proved that adjusting the pH or net charges of the amino acid sequences can promote or inhibit the self-assembly of β-sheets into amyloid fibers.

1.3 Natural peptide self assembly utilized by insects

Functional amyloids are found to be implemented naturally by several different organisms. Insects are able to produce silk for many purposes. Silkworms such as the *Bombyx mori* produce silk for cocoons [14]. Researchers have recently shown greater interest in silk because it has excellent mechanical properties and because of its proteinaceous composition. Spiders produce dragline silk to ascend and descend that has high tensile strength and is mechanically rigid [14,15]. Obviously, each silk producing insect has different uses for its silk but the common denominator is the extrusion mechanism in which the silk is produced. The extrusion or "spinning" process from the insect aligns the protein chains parallel to the fiber axis producing the most common β-sheet structure in nature. Regions of semi-crystallinity (the hydrogen bound β-sheets) and amorphous matrices provide packing efficiency and contribute to strength. In rarer cases, some insects produce silk that contains cross-β fibers. The cross-β structure is achieved in the absence of extrusion but produces a material with similar semi-crystalline and amorphous regions and mechanical properties to the natural β-sheet structure [15]. A protein solution is simply deposited by the insect and upon drying produces a micron-sized cross-β fiber through a self-assembly process. The most fascinating phenomenon

of silk production is the transition of liquid to solid phases. Insects store aqueous solutions of silk proteins and when prompted the silk emerges from the gland as a fiber. When the insect is ready to extrude its silk, a drop of the liquid is released and then it slowly pulls away to construct the web or cocoon. As the silk thread elongates from the extrusion gland of the insect, the shear forces assist in the alignment of peptide bonds. The β-sheet structure is achieved by formation of peptide bonds and the relocation of hydrophobic regions that dismiss water and allow for the production of mechanically tensile silk thread [14]. High concentration of proteins yields high viscosity [14]. Protein alignment in the fiber structure is due to an applied pressure and the ordered crystalline regions are subject to protein concentration, which also affects viscosity. If the viscosity is high, it will prevent capillary break-up during extrusion [14]. Much less is known about the simple deposition process utilized by insects that form cross-β fibers. From our own observations, the liquid to solid transition or drying of the water from the fiber appears to only be important in allowing enough protein molecules to self-assemble to form a micron-sized fiber, i.e., is a concentration effect.

1.4 Functional vs. Pathogenic Amyloids

The two categories of amyloids are functional and pathogenic. Pathogenic amyloids are cross-β fiber aggregates that are responsible for neurodegenerative diseases in animals and humans. This group includes: Type II diabetes, Alzheimer's, scrapie, and Huntington diseases, for instance. Fibril formation extracellularly arises when the protein systems or peptides change and aggregate to an insoluble state[1]. The aggregates accumulate and cause amyloidosis. Amyloidosis is characterized by the presence of amyloid fibers. The

robust cross-β structure of amyloids makes them insoluble in water. Human bodies are made up of about 60% water and this property is extremely vital to the promotion of aggregation and further elevation of prion diseases. Prion diseases are another group of neurodegenerative diseases that include spongiform encephalopathies [1]. Prion proteins associated with this set of diseases cause an aggregated plaque build-up in the brain. These plaques destroy neurons. The two types of prion proteins responsible for prion diseases are prion-protein cellular (PrP^{C}) and prion protein-scrapie (PrP^{Sc}) [2]. Although these diseases have varying symptoms, the common cause of neurodegeneration is due to extracellular protein aggregation [9,10,16,17].

The prion proteins exist in the two types but only PrP^{Sc} is harmful. PrP^{C} does not form extracelluar amyloid plaques unless prompted. PrP^{Sc} can aggregate extracellularly and ignite the conversion of PrP^{C} to PrP^{Sc}. This transition and the role of the PrP^{C} remain undefined [2].

The protein linked to Alzheimer's disease is the amyloid-β (Aβ) protein. Pawar *et al*. researched the "aggregation propensity profile" of the amyloid-β protein (Aβ) [18]. Researchers hoped that the creation of the propensity profile would help predict the sequence or location of amyloid aggregation. Properties that effect aggregation are pH, temperature, amino acid sequence, and concentration. The propensity profile of Aβ42 was examined within a 2-9 pH range. The profiles were more independent within the 4.5-9 pH range. Results were compared to NMR results of solid-state amyloid fiber aggregation and were in agreement. The identification of the "aggregation prone" region

was obtained from the high success of the profile and is believed to be the region that assists the amino acid sequence in aggregation.

Another region, the “aggregation susceptible” region, was determined through adjustments in the profile due to mutations. Amino acid mutations can positively or negatively impact the propensity profile, which directly correlates to the “aggregation susceptible” region [18]. The research of these regions is important in determining the susceptibility and likelihood of neurodegenerative diseases. There is a host of studies dedicated to this biological mechanism of extracellular aggregation.

Determining the mechanism for extracellular fibril formation is helpful for the discovery and advancement of functional amyloids as biological nanomaterials. Nanomaterial adaptability to various environments is the major obstacle for this subject of material science. Once this hurdle is achieved, self-assembled materials can be considered for a wide range of applications [19,20]. This is due to the materials’ ability to adopt different chemical changes, size, and outstanding physical properties [20]. Through these advancements the functionality of self-assembled amyloids can be implemented to making biological nanomaterials. The route of protein self-assembly is more intriguing when we know the time scale in which the systems assemble.

1.5 Environmental Impacts

Environmental, health, and societal effects can be impacted through research of functional amyloids. Industrial processes rely heavily on fossil fuel inputs for feedstocks

and energy. Process energy comes from fossil fuels like coal, natural gas, or petroleum. The mining of these resources wreaks havoc on the surrounding environment usually releasing large amounts of heavy metals, sulfur, methane, carbon dioxide, and nitrous oxide. Fossil resources are usually mined in environmentally sensitive areas such as the ocean (petroleum and natural gas) or a mountain (coal) and results in the destruction of the natural setting and impacting vegetation and wildlife. The release of green house gases (GHG) and the aforementioned compounds in both their natural and acidic forms additionally destroy vegetation, water quality, and wildlife above and beyond the physical destruction of the landscape with machines [21]. Mining is a very dangerous occupation putting miners at risk for respiratory diseases and subjecting them to the dangers of the heavy equipment required for fossil fuel removal. The combustion of fossil fuels for process energy results in the release of GHG, sulfur, and nitrogen compounds into the atmosphere further degrading air quality.

In the petrochemical industry, the product itself can become a nuisance because it is hydrocarbon-based and not easily biodegraded in the environment. According to the EPA, about 12% of municipal solid waste (MSW) is plastic packaging currently taking up space in a landfill [22]. Making products from biological sources like peptides allows for robust materials that can eventually be biodegraded. For instance, the human body has fully functional materials that are stable during use but can eventually be biodegraded. Plastic not properly disposed has followed ocean currents to “dead zones” where plastic debris has heavily accumulated [23].

Some studies have found statistical links between industrialization and adverse health effects. Industrialized areas have been correlated to increased incidents of multiple sclerosis and child mortality [24, 25]. While industrialization increases incomes and allows people financial and physical access to health care it also seems to have the adverse effect of polluting the local environment and degrading human health. Production and use of functional amyloids as biodegradable materials can be utilized as an alternative to the previously listed environmental issues.

Efforts are underway to utilize biological feedstocks for fuels, chemicals, and plastics. Most focus on replacing petroleum or natural gas with a biological input [26]. Some are focused on "bioprocessing" which is to rely on more benign biological systems to do the work of making a product from biomass. We are focused on a very unique form of bioprocessing relying on spontaneous thermodynamic processes in nature. The scientific importance of my work is to utilize renewable resources like plant proteins processed in low energy ways using nature's preferred thermodynamics. The societal importance is that, in taking advantage of highly efficient biological processes that have evolved over millennia, there is no need for large amounts of process energy in the form of combusted fossil fuels and no need for organic solvents obtained from petroleum. The associated harmful environmental and health effects from fossil fuel use are also eliminated.

1.6 Peptide Self-assembly Over Many Length Scales

Self-assembly is very complex on the nanoscale but we aim to prove the macroscopic elevation of a protein system that can allow us to further investigate peptide self-

assembly and aggregation [3,4,20]. It is my goal to examine the protein system in an aqueous environment using attenuated total reflectance (ATR)-FTIR spectroscopy. Goormaghtigh *et al.* evaluated protein secondary structure using circular dichroism (CD), transmission, and ATR-FTIR [27]. Qualitative information obtained was similar but ATR-FTIR results were more intense and specific. Using ATR-FTIR, a larger group of protein features can be classified especially relating specific Amide I bands to secondary structure [27].

Ishida and Griffiths compared the Amide I and Amide II intensity ratios in β-lactoglobulin, myoglobin, and albumin using ATR-FTIR, transmission, and diffuse reflectance spectroscopies [32]. The intensity ratios of the amide I region were significantly different for proteins in aqueous solution compared to the solid-state proteins. The change in intensity ratios is a factor of examining the proteins in two different states. It is more difficult to obtain information from a protein film because of it's absorbance to the surface. Proteins in solution can provide more structural information and show greater intensity when scanned [32].

Because of the perseverance of structure, ATR-FTIR was used by Oberg *et al.* to determine the structure of proteins in inclusion bodies and other forms of protein aggregation [29]. It was determined that the three aggregated forms were: inclusion bodies, aggregates formed during thermal denaturation, and aggregates formed during refolding from denaturant. The amount of secondary structures in the control was the same for the amount of secondary structures identified in the inclusion bodies. Inclusion

bodies are cells that harbor proteins internally [33]. We did not examine proteins within inclusion bodies but this shows the versatility of ATR-FTIR.

1.6.1 Research Objectives

My approach was to utilize natural, biological sources for materials and low energy biological processes to make them.

Objective 1: Understand peptide self-assembly mechanism.

The research in our group has corroborated what has been observed in other groups, that it is possible to self-assemble nanofibers and crystals from peptides that can be used as high modulus materials. Unique to our research is the ability to self-assemble a micron-sized peptide fiber like that shown in Figure 1 from common proteins, like abundant plant proteins.

Objective 2: Identify structure of self-assembled fibers.

We will successfully identify the structure evolution of the fibers using attenuated total reflectance Fourier transform infrared spectroscopy (ATR-FTIR).

1.6.2 Hypothesis

Large fibers form spontaneously from a long α-helix adder peptide and a short hydrophobic β-sheet template peptide. When mixed, fibers form as hydrophobic groups

on the template peptide find each other and inter-molecularly hydrogen bond through main chain interactions to form stable β-sheets. Adder peptides undergo α to β transitions on the template and allow further β-sheet formation. This is the attainment of a first equilibrium resulting in an "elementary unit". Fiber formation can continue as remaining peptides find the first equilibrium structure in the changing solution and aggregate with it, reaching another equilibrium.

1.7 References

[1] AM Lesk, Introduction to Protein Science-Architecture, Function, and Genomics, 1st ed., Oxford University Press, New York, NY, 2004.

[2] U Langel, BF Cravatt, A Graslund, G von Heijne, T Land, S Niessen, et al., Introduction to Peptides and Proteins, CRC Press Taylor & Francis Group, Boca Raton, FL, 2010.

[3] F Chiti, CM Dobson. Protein Misfolding,Functional Amyloid, and Human Disease, Annual Review of Biochemistry. 75 (2006) 333-366.

[4] Ahmad I Athamneh and Justin,R.Barone, Enzyme-mediated self-assembly of highly ordered structures from disordered proteins, Smart Mater.Struct. 18 (2009) 104024.

[5] VN Uversky, AL Fink. Conformational constraints for amyloid fibrillation: the importance of being unfolded, Biochimica et Biophysica Acta (BBA) - Proteins & Proteomics. 1698 (2004) 131-153.

[6] CM Dobson. Protein folding and misfolding, Nature. 426 (2003) 884-890.

[7] A Sethuraman, G Vedantham, T Imoto, T Przybycien, G Belfort. Protein Unfolding at Interfaces: Slow Dynamics of α-Helix to β-Sheet Transition, PROTEINS: Structure, Function, and Bioinformatics. 56 (2004) 669-678.

[8] E Gazit. Self-assembled peptide nanostructures: the design of molecular building blocks and their technological utilization, Chemical Society Review. 36 (2006) 1263-1269.

[9] R Pellarin, A Caflisch. Interpreting the Aggregation Kinetics of Amyloid Peptides, J.Mol.Biol. 360 (2006) 882-892.

[10] AT Petkova, RD Leapman, Z Guo, W Yau, MP Mattson, R Tycko. Self-Propagating, Molecular-Level Polymorphism in Alzheimer's ß-Amyloid Fibrils, Science. 307 (2005) 262-265.

[11] RM Murphy. Kinetics of amyloid formation and membrane interaction with amyloidogenic proteins, Biochimica et Biophysica Acta (BBA) - Biomembranes. 1768 (2007) 1923-1934.

[12] CL Masters, G Simms, NA Weinman, G Multhaup, BL McDonald, K Beyreuther. Amyloid plaque core protein in Alzheimer disease and Down syndrome, Proceedings of the National Academy of Sciences of the United States of America. 82 (1985) 4245-4249.

[13] M López de la Paz, K Goldie, J Zurdo, E Lacroix, CM Dobson, A Hoenger, et al. De novo designed peptide-based amyloid fibrils, Proceedings of the National Academy of Sciences of the United States of America. 99 (2002) 16052-16057.

[14] S Weisman, S Okada, ST Mudie, MG Huson, HE Trueman, A Sriskantha, et al. Fifty years later: The sequence, structure and function of lacewing cross-beta silk, Journal of Structural Biology. 168 (2009) 467-475.

[15] TD Sutherland, JH Young, S Weisman, CY Hayashi, DJ Merritt. Insect Silk: One Name, Many Materials, Annual Review of Entomolgy. 55 (2010) 171-188.

[16] AT Petkova, Y Ishii, JJ Balbach, ON Antzutkin, RD Leapman, F Delaglio, et al. A structural model for Alzheimer's β-amyloid fibrils based on experimental constraints from solid state NMR, Proceedings of the National Academy of Sciences of the United States of America. 99 (2002) 16742-16747.

[17] F Rousseau, J Schymkowitz, L Serrano. Protein aggregation and amyloidosis: confusion of the kinds? Curr.Opin.Struct.Biol. 16 (2006) 118-126.

[18] AP Pawar, KF DuBay, J Zurdo, F Chiti, M Vendruscolo, CM Dobson. Prediction of "Aggregation-prone" and "Aggregation-susceptible" Regions in Proteins Associated with Neurodegenerative Diseases, J.Mol.Biol. 350 (2005) 379-392.

[19] K Sanford, M Kumar. New proteins in a materials world, Current Opinion in Biotechnology. 16 (2005) 416-421.

[20] K Channon, CE MacPhee.Possibilities for 'smart' materials exploiting the self-assembly of polypeptides into fibrils, Soft Matter. 4 (2008) 647-652.

[21] DA Nimick, SE Church, SE Finger, Intergrated investigations of environmental effects of historical mining in the Basin and Boulder Mining Districts,Boulder River Watershed, Jefferson County Montana, U.S. Geological Survey Professional Paper 1652 (2004).

[22] US EPA, Municipal Solid Waste in the United States: Facts and Figures | Municipal Solid Waste | Wastes | US EPA, 2011.

[23] RC Thompson, Y Olsen, RP Mitchell, A Davis, SJ Rowland, AWG John, et al. Lost at Sea: Where Is All the Plastic? Science. 304 (2004) 838-838.

[24] G Rosati. The prevalence of multiple sclerosis in the world: an update, Neurological Sciences. 22 (2001) 117.

[25] M Federman, D Levine, Industrialization and infant mortality, (2004).

[26] JH Clark, F Deswarte, Introduction to chemicals from biomass, Wiley and Sons, Ltd., Chichester, 2008, pp. 198.

[27] E Goormaghtigh, V Raussens, J Ruysschaert. Attenuated total reflection infrared spectroscopy of proteins and lipids in biological membranes, Biochimica et Biophysica Acta. 1422 (1999) 105-185.

[28] KA Oberg, AL Fink. A New Attenuated Total Reflectance Fourier Transform Infrared Spectroscopy Method for the Study of Proteins in Solution, Anal.Biochem. 256 (1998) 92-106.

[29] K Oberg, BA Chrunyk, R Wetzel, AL Fink. Native-like Secondary Structure in Interleukin-1.beta. Inclusion Bodies by Attenuated Total Reflectance FTIR, Biochemistry(ACS). 33 (1994) 2628-2634.

[30] C Vigano, L Manciu, F Buyse, E Goormaghtigh, J- Ruysschaert. Attenuated total reflection IR spectroscopy as a tool to investigate the structure, orientation and tertiary structure changes in peptides and membrane proteins, Peptide Science. 55 (2000) 373-380.

[31] AR Hind, SK Bhargava, A McKinnon. At the solid/liquid interface: FTIR/ATR — the tool of choice, Adv.Colloid Interface Sci. 93 (2001) 91-114.

[32] KP Ishida, PR Griffiths. Comparison of the Amide I/II Intensity Ratio of Solution and Solid-State Proteins Sampled by Transmission, Attenuated Total Reflectance, and Diffuse Reflectance Spectrometry, Applied Spectroscopy. 47 (1993) 584-589.

[33] RR Kopito. Aggresomes, inclusion bodies and protein aggregation, Trends Cell Biol. 10 (2000) 524-530.

[34] A Athamneh, Peptide self-assembly from the molecular to the macroscopic scale at standard conditions, University Libraries, Virginia Polytechnic Institute and State University. (2010) 1-147.

Chapter 2: Examination of Self-assembly

2.1 Materials

Gliadin, myoglobin, and trypsin were obtained from Sigma-Aldrich (USA). Trypsin was the enzyme of choice for proteolysis of gliadin. Myoglobin is a respiratory protein found in muscles of animals and humans with two subunits, heme and globin [1,2]. It is approximately 75% α-helix [2]. Non-polar groups present in its structure are protected internally by polar and charged groups on the surface. Gliadin is an alcohol soluble component of wheat gluten [3].

2.1.1 Fourier Transform-Infrared Spectroscopy

Analysis of aggregation in solution was done using the Thermo Scientific Nicolet 6700 FTIR spectrometer with an ATR ZnSe 45˚ crystal. Two hundred and fifty six scans were taken three times for every sampling time. Background scans were taken before each sample. IR spectroscopy is advantageous because of time efficiency and it has a wide application range for self-assembled systems. Spectroscopy techniques make it easy to examine proteins in solutions [4-7]. ATR allows for the examination of protein secondary structure in the native environment [5-7]. With an approximate sample size of 1 mL, we get rapid results and strong signals. For our system, using a demountable liquid cell was problematic because of the confined cell space that was of the same magnitude as the produced fibrous protein aggregate. By examining the protein system in a larger volume aqueous environment using ATR-FTIR we are able to see changes in the Amide I, Amide II, and aliphatic regions quickly and the integrity of the system was preserved [4,6,7].

To determine specific secondary structures present in solutions, IR spectroscopy yields useful information about the amide and aliphatic groups. We analyzed the Amide I region (1600-1700 cm^{-1}), Amide II (1510-1550 cm^{-1}), and aliphatic (1350-1415 cm^{-1}) absorbances to examine the kinetics of the assembling myoglobin and gliadin systems. The Amide I region represents the carbonyl (C=O) stretching. The Amide I absorbance is highly dependent on the absence or presence of secondary structures [8]. The Amide II region represents the carbon and nitrogen (C-N) in the peptide bond. All amino acids have this in common so it is expected in all IR spectra of proteins. Amide I and II changes represent changes in hydrogen bonding in the system. For the case of self-assembly, this is usually the gain of inter-molecular hydrogen bonding in very specific patterns related to the gain of secondary structure. The aliphatic region represents the deformations of the CH_2 and CH_3 groups on amino acid side chains. Information from the aliphatic region relates to hydrophobic interactions between peptide molecules. Hydrogen bonds are the strongest bonds within our systems and they play an important role in structure breakdown and self-assembly. IR spectroscopy is also more versatile compared to other techniques, i.e. samples can be solid or liquid and they do not have to be "optically transparent" [9,10].

We studied the kinetics of peptide aggregation as a function of the ratio of the two proteins mixed in the system. The percentages of myoglobin (α-helix) present in solution with gliadin (β-sheet template) were: 0, 25, 50, 75, and 100%.

2.2 Methods

2.2.1 Hydrolysis

60 mg of trypsin was dissolved into 800 mL of pure H_2O. Then, 20 g of gliadin was slowly added for a liquid to solids ratio of 25 mg/mL. The solution was stirred for 72 hours at 37˚C with pH manually adjusted to 8 using 0.01M HCl. The solution was poured onto Teflon coated aluminum foil to dry before use. Trypsin cleaves proteins at arginine (R) and lysine (K) except when either is next to a bulky proline (P) amino acid.

2.2.2 Peptide/protein mixtures

Into 10 ml of pure H_2O, a total solids content of 250 mg of myoglobin and hydrolyzed gliadin was added in varying ratios. The 1:1 ratio had equal weights of 125 mg. In the case of the 1:3 ratio 62.5 mg of gliadin was mixed with 187.5 mg of myoglobin and vice versa for the 3:1 ratio.

The pH of each system was manually adjusted to 8 with 0.025M NaOH and 0.01M HCl immediately at the start. It was monitored for the duration of the experiments. We analyzed the mixtures in FT-IR every 2 hours on day 1, 3 times a day on the next day, and then once a day in the following two weeks. In between scans, the solutions incubated in the oven at 37˚C.

2.2.3 Deconvolution

It is well accepted that deconvolution of the Amide I absorbance can reveal intricate details about protein secondary structure [11]. Each secondary structure has a definitive Amide I absorbance as shown in Table 1. The cross-β structure specifically shows up at 1621 cm^{-1} [8,12] Therefore, by treating the Amide I band as a summation of these

absorbances, we can calculate the relative amounts of each in the mixtures. This is important because we have demonstrated from previous laboratory results that the self-assembled fibers possess the cross-β secondary structure and we hypothesize that it forms at least partially from one of the proteins or peptides in the mixture undergoing an α to β transition. So we can directly monitor any loss of α-helix and gain of β-sheet. Amide I absorbances were deconvoluted using Omnic Software v. 7.4. IR spectra were baseline corrected and peak resolved with a low sensitivity using 3.857 full width at half height (FWHH), a target noise of 10, and a linear baseline. Gaussian-Lorentzian was the chosen peak plotting output. Thus, the Amide I band was fit to a sum of Gaussian/Lorentzian functions with each representing one of the identified protein secondary structures. For each experiment, three scans were taken and deconvoluted so the amount of secondary structure was presented as an average with standard deviation. The fraction of each secondary structure was calculated:

Equation 1 Determination of beta fractions within the protein systems

$$\text{Total Beta} = \beta_T = \text{cross } \beta + \beta \text{ sheet}$$

$$\text{Beta Fraction} = \frac{\beta_T}{\beta_T + random + \alpha\ helix}$$

2.1 References

[1] M Fändrich, V Forge, K Buder, M Kittler, CM Dobson, S Diekmann. Myoglobin forms amyloid fibrils by association of unfolded polypeptide segments, Proceedings of the National Academy of Sciences of the United States of America. 100 (2003) 15463-15468.

[2] LJ Kagen, Myoglobin; Biochemical, Physiological, and Clinical Aspects, 1st ed., Columbia University Press, New York, NY, 1973.

[3] A Fasano, R Troncone, D Branski, Pediatric and Adolescent Medicine, Frontiers in Celiac Disease, 1st ed., Karger, New York, NY, 2008, pp. 222.

[4] AR Hind, SK Bhargava, A McKinnon. At the solid/liquid interface: FTIR/ATR — the tool of choice, Adv.Colloid Interface Sci. 93 (2001) 91-114.

[5] E Goormaghtigh, V Raussens, J Ruysschaert. Attenuated total reflection infrared spectroscopy of proteins and lipids in biological membranes, Biochimica et Biophysica Acta. 1422 (1999) 105-185.

[6] KA Oberg, AL Fink. A New Attenuated Total Reflectance Fourier Transform Infrared Spectroscopy Method for the Study of Proteins in Solution, Anal.Biochem. 256 (1998) 92-106.

[7] K Oberg, BA Chrunyk, R Wetzel, AL Fink. Native-like Secondary Structure in Interleukin-1.beta. Inclusion Bodies by Attenuated Total Reflectance FTIR, Biochemistry(ACS). 33 (1994) 2628-2634.

[8] H Gunzler, H Gremlich, IR Spectroscopy, Wiley-VCH, Weinheim, 2002.

[9] DR Brown, Neurodegeneration and prion disease, 1st ed., Springer, New York, NY, 2005, pp. 473.

[10] U Langel, BF Cravatt, A Graslund, G von Heijne, T Land, S Niessen, et al., Introduction to Peptides and Proteins, CRC Press Taylor & Francis Group, Boca Raton, FL, 2010.

[11] S Wi, P Pancoska, TA Keiderling. Prediction of protein secondary structures using factor analysis on Fourier transform infrared spectra: Effect of Fourier self-deconvolution of the amide I and amide II bands, Biospectroscopy. 4 (1997) 93-106.

[12] Z Ganim, HS Chung, AW Smith, LP DeFlores, KC Jones, A Tokmakoff. Amide I Two-Dimensional Infrared Spectroscopy of Proteins, Acc.Chem.Res. 41 (2008) 432-441.

Chapter 3: Results and Discussion

3.1 Results

Figure 3 shows that round fibers resulted from mixtures with high gliadin (template) content and flat tapes resulted from mixtures with high myoglobin (adder) content. Higher magnification scanning electron micrographs of the large fibers can be seen in Figure 1 also showing the transition from round (high gliadin content) to flat (high myoglobin content) fiber shape. It was observed that fibers could be 1-2 mm long (Figure 1(b)) and some had an intrinsic twist to them (Figure 1(c)).

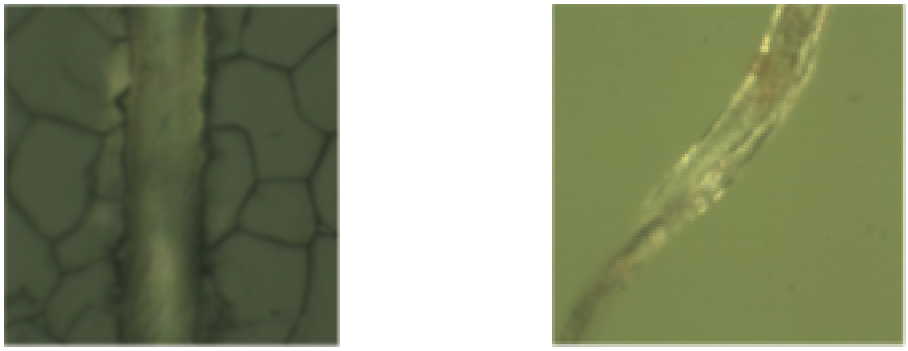

(a) (b)

Figure 3 Optical microscopy pictures of fibers with (a) high hydrolyzed gliadin and (b) high myoglobin content. Fibers are 10 μm across.

The Amide I absorbance, centered around 1640 cm^{-1}, was deconvoluted into the following principal protein secondary structure components. The components are listed in Table 1.

Table 1 Deconvolution absorbances for the protein secondary structures within the systems

Secondary Structure Component	Absorbance (cm^{-1})
cross-β	1617-1625
β-sheet	1630-1638
α-helix	1645
random coil	1652
β-turn	1662-1668
anti-parallel β-sheet	1683

So each of these components was represented by a Gaussian/Lorentzian function and the total Amide I absorbance was fit to a combination of these absorbances to yield the fraction of each component or the "deconvolution". The major protein secondary structure components were the β-sheet, α-helix, and random coil. The anti-parallel β-sheet absorbance was used to tell how much of the β-sheets were in the anti-parallel configuration versus the parallel configuration. The β-turn is a minor fraction for most common proteins and was a negligible fraction in the analysis. The cross-β is a very uncommon secondary structure as noted in the Introduction but forms in our systems and we have determined it to be prominent. Since this is a fitting procedure and there is some subjectivity involved in assigning the exact absorbances, we defined total β-structures as the fraction of cross-β plus the fraction of β-sheet determined from the deconvolution, represented as β_T (i.e., β_T = cross-β + β-sheet). However, the major structures, β-sheet,

α-helix, and random coil, appear far enough apart in their pure forms to be confident that the deconvolution can separate the three [4-5]. From the deconvolution results, the secondary structure fractions were represented as:

$$\beta_T = \frac{\beta_T}{\beta_T + \alpha + rc} \qquad \alpha = \frac{\alpha}{\beta_T + \alpha + rc} \qquad rc = \frac{rc}{\beta_T + \alpha + rc}$$

where rc is random coil and $\beta_T + \alpha + rc = 1$.

3.1.1 0% Gliadin & 100% Myoglobin (Gd:My 0:1)

Figure 5 shows the change in the secondary structure fractions for the Gd:My 0:1 mixture. In general, there was no significant change in the secondary structure and no fibers were observed.

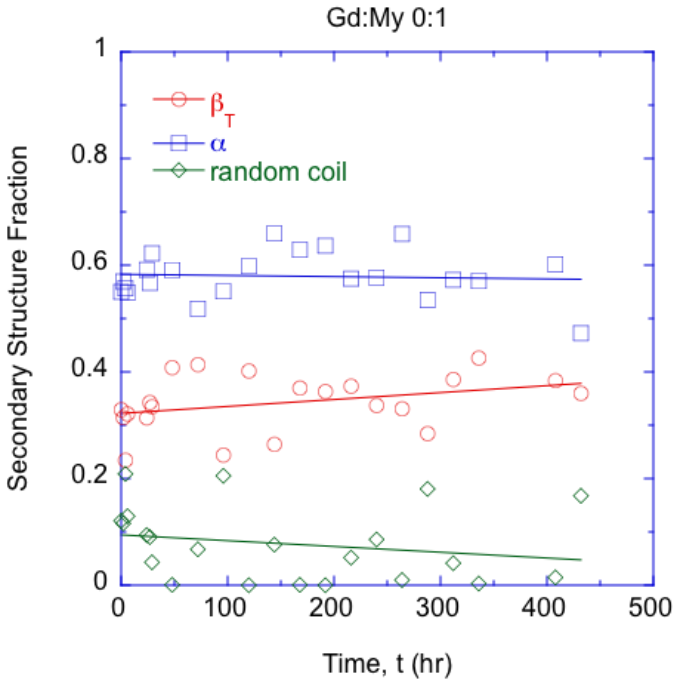

Figure 4 Secondary structure fractions for each of the secondary structures present within the 0:1 system

Figure 4 shows the changes in protein secondary structure as determined through Amide I deconvolution. The changes in the Amide I, Amide II, and aliphatic regions of the Gd:My 0:1 system for various points in time are plotted in Figures 5-8.

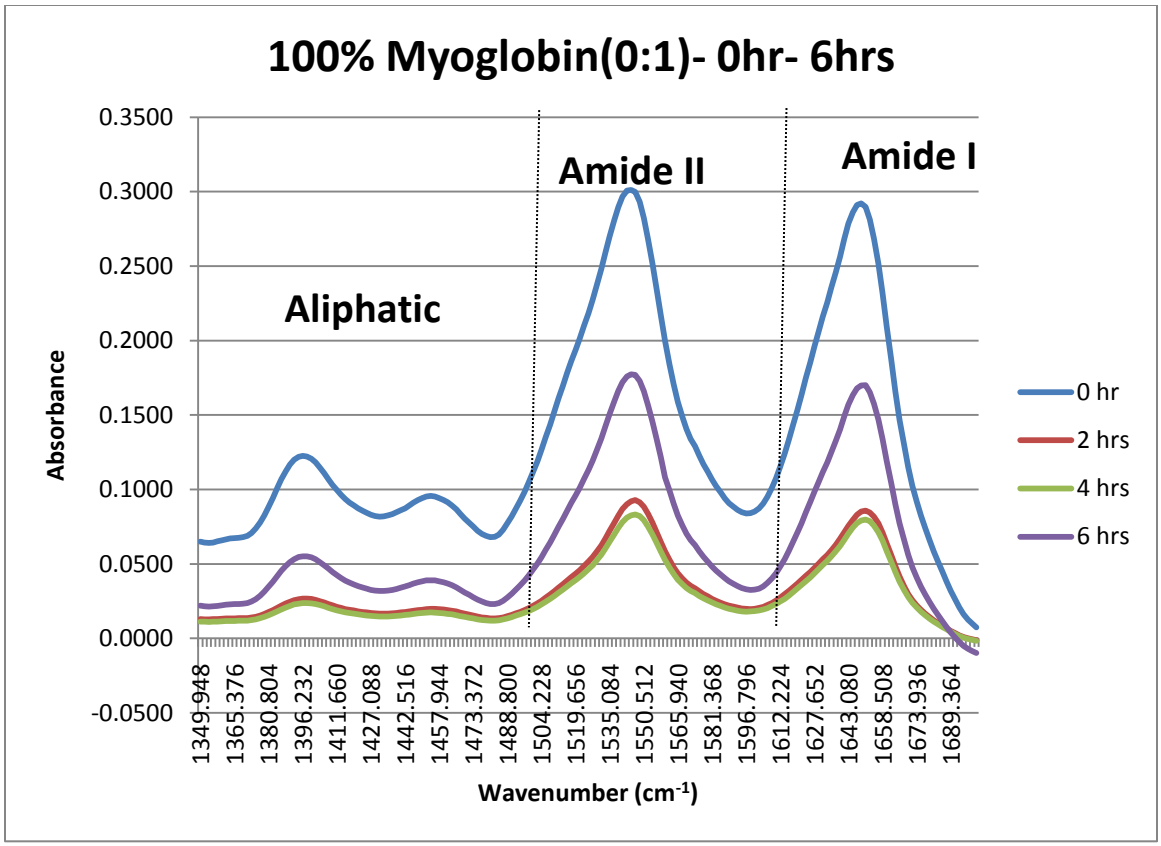

Figure 5 Gd:My 0:1 system during the first 6 hours

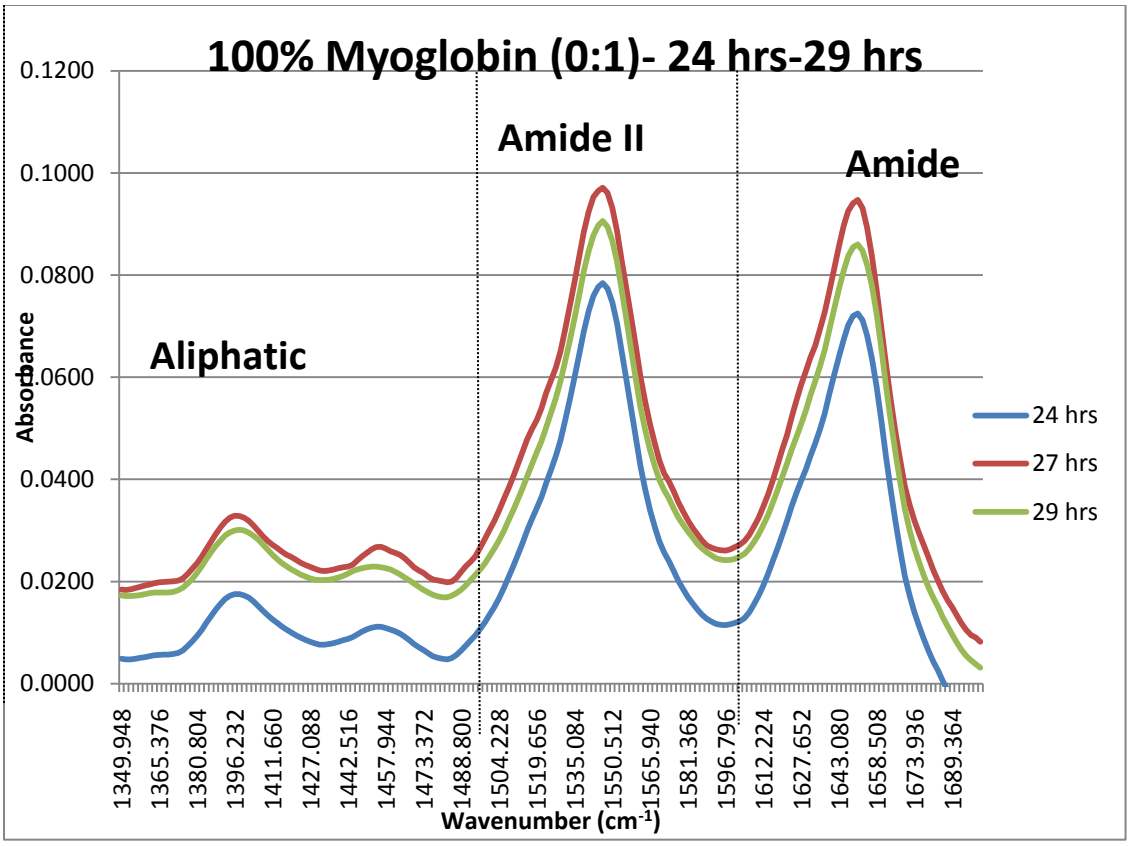

Figure 6 Gd:My 0:1 system within the first 24 hours

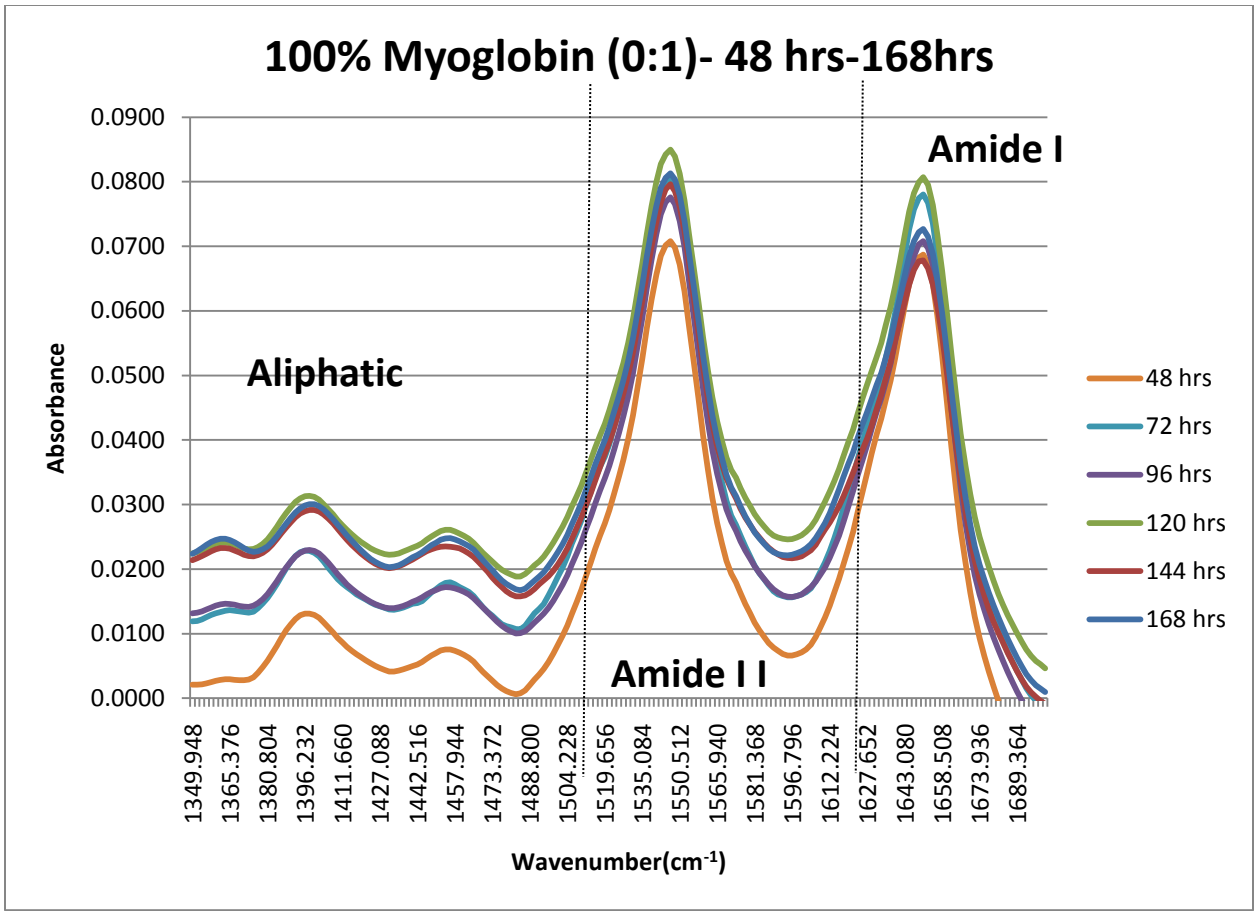

Figure 7 Gd:My 0:1 system during week 1

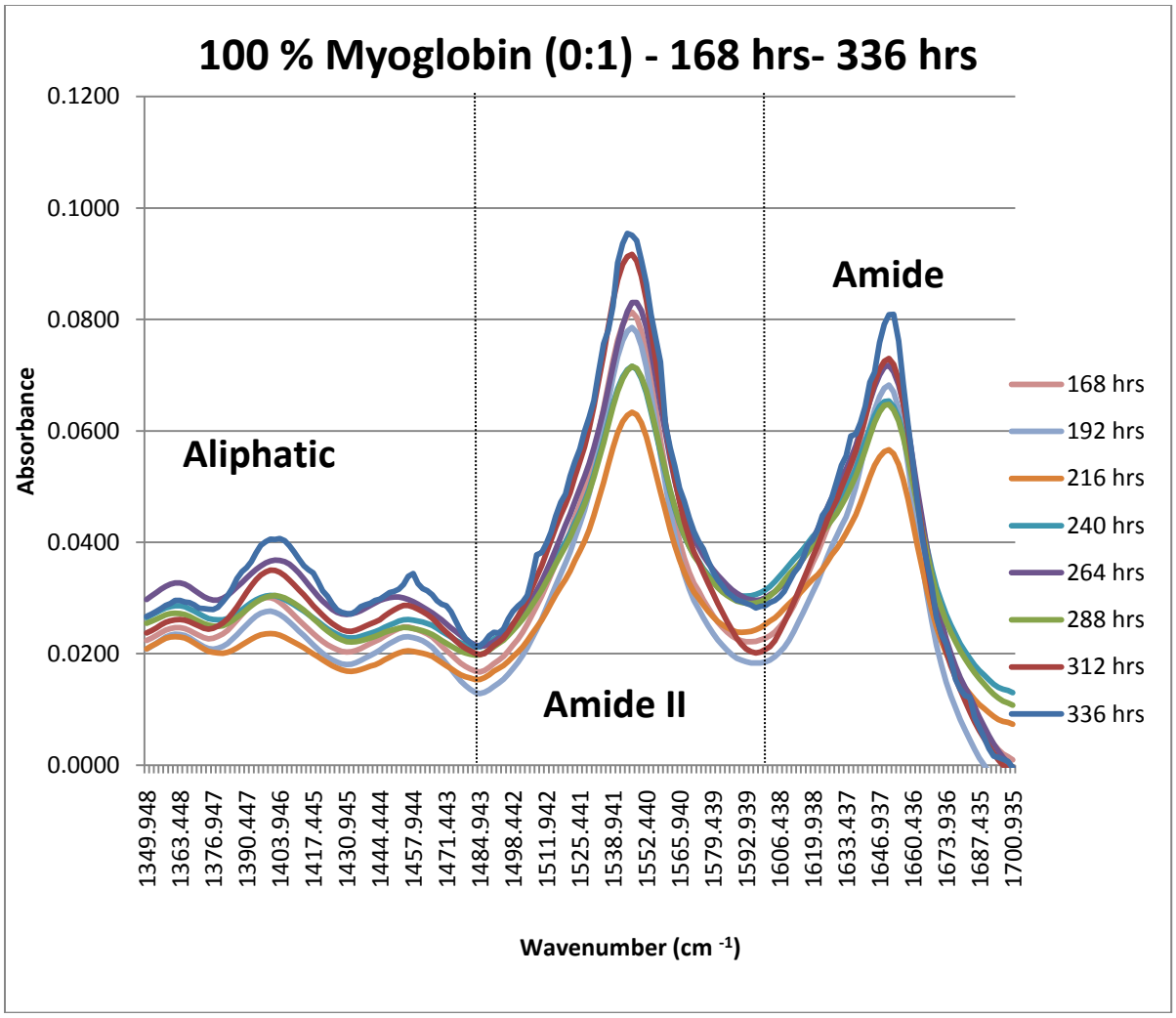

Figure 8 Gd:My 0:1 system during week 2

3.1.2 25% Gliadin & 75% Myoglobin (Gd:My 1:3)

When a minor fraction of hydrolyzed gliadin (Gd) was added to myoglobin (My), 25% (Gd:My 1:3), there was a much larger change in the secondary structure (Figure 9), specifically the β_T and α fractions. The change in secondary structure continued over all time and the amount of total β-structures gained (β_T) was approximately the amount of α-helices lost. There was no change in the random coil fraction.

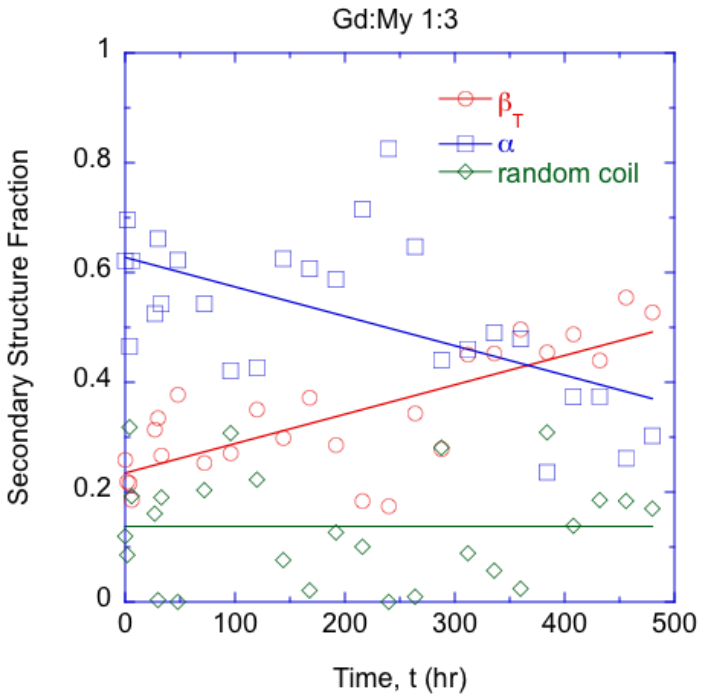

Figure 9 Secondary structure fractions for each of the secondary structures present within the Gd:My 1:3 system

Figures 10-13 show changes in the amide I, amide II, and aliphatic regions for the Gd:My 1:3 system.

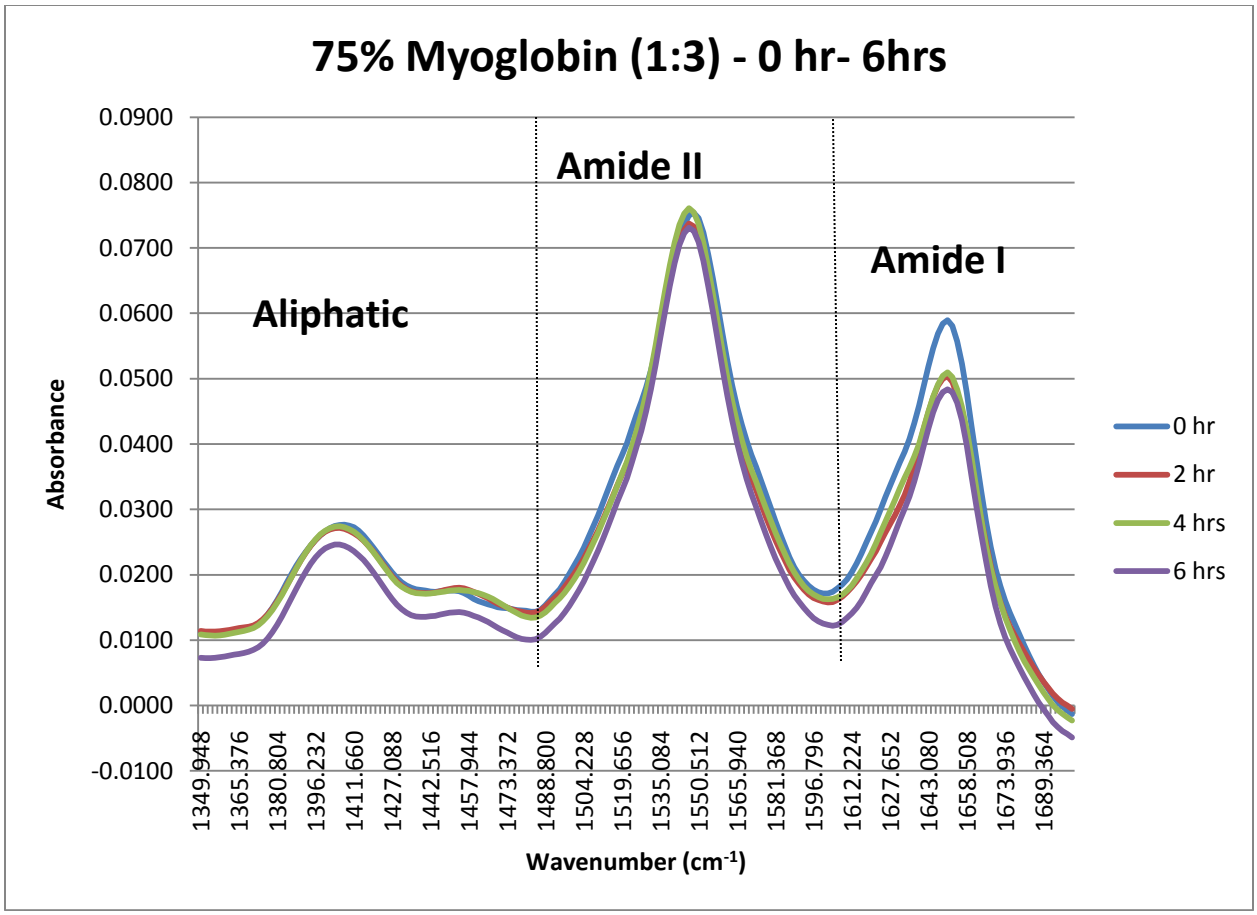

Figure 10 Gd:My 1:3 system during the first 6 hours

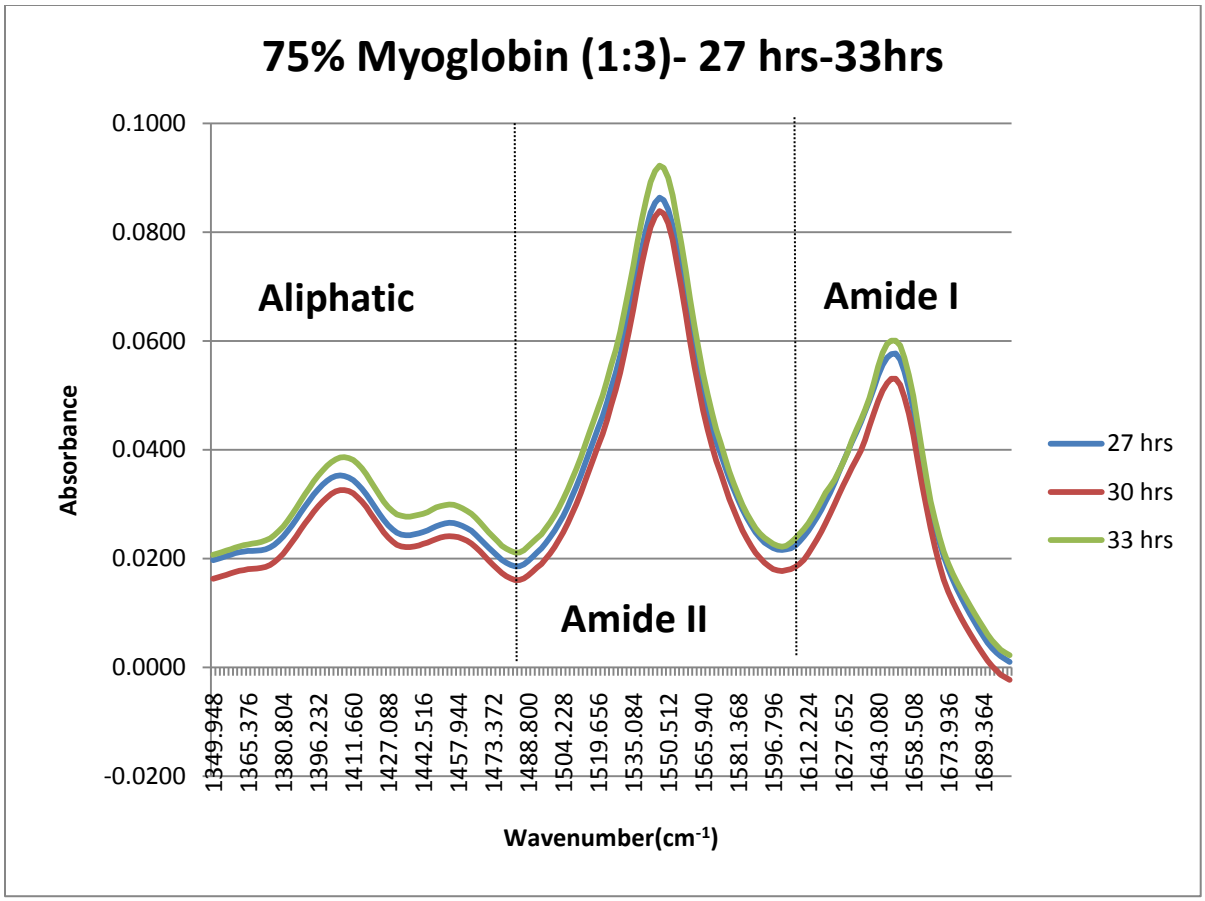

Figure 11 Gd:My 1:3 system shortly after 24 hours

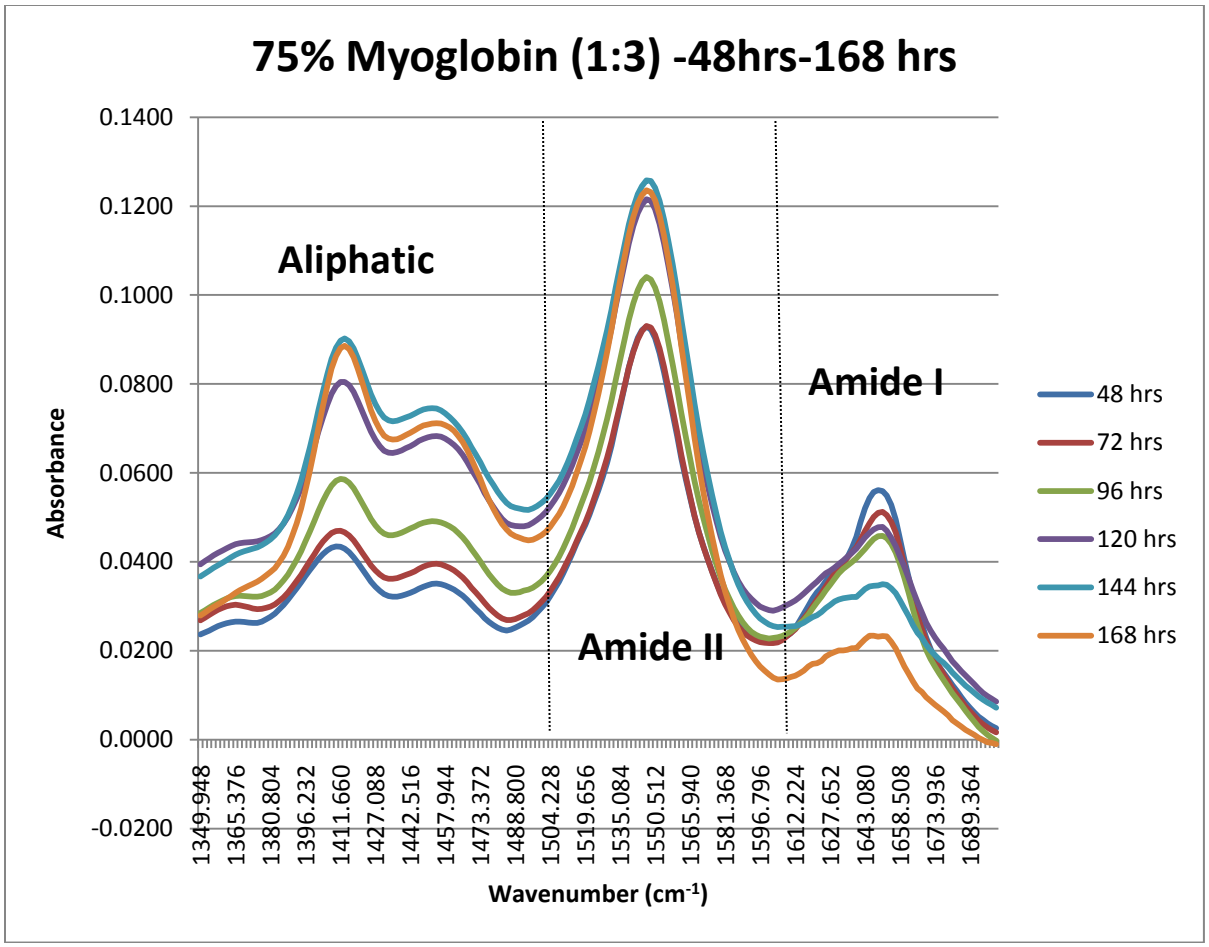

Figure 12 Gd:My1:3 system during week 1

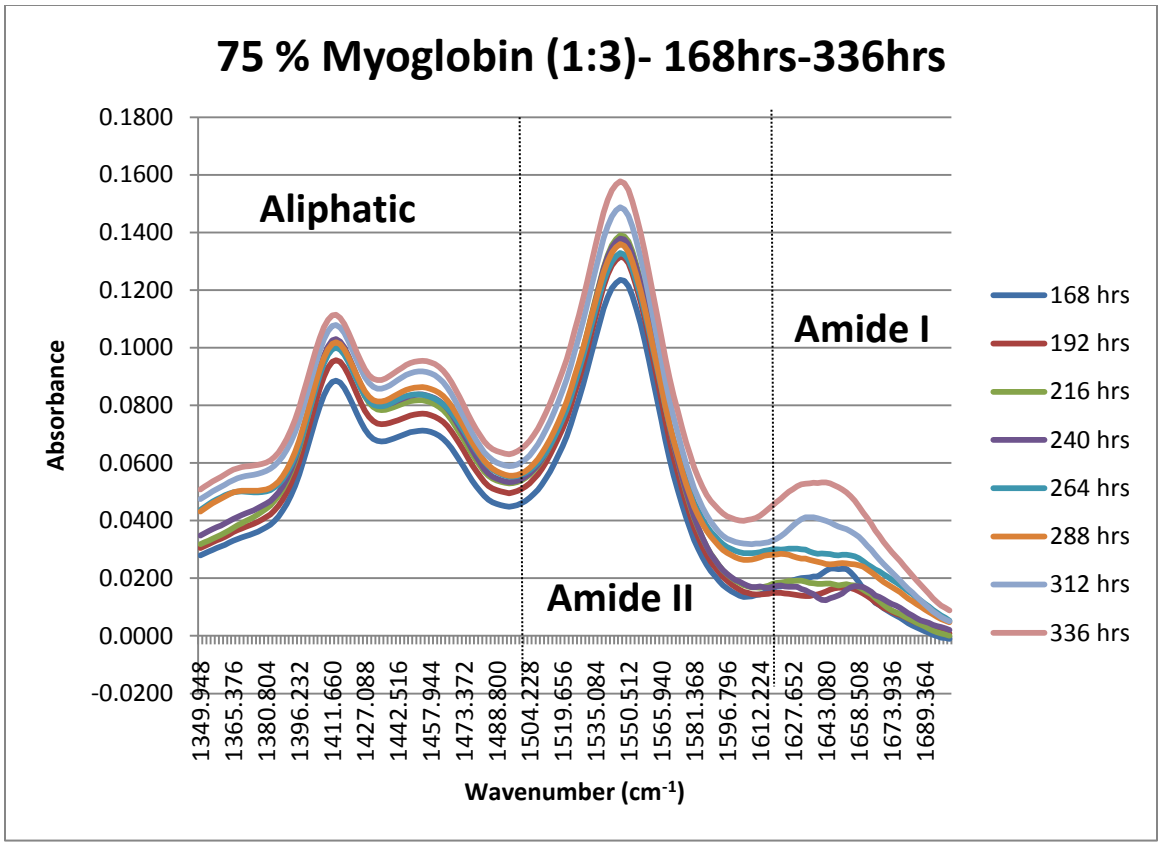

Figure 13 Gd:My 1:3 system during week 2

3.1.3 50% Hydrolyzed Gliadin and 50 % Myoglobin (Gd:My 1:1)

The addition of Gd in equal mass fraction to My, Gd:My 1:1, produced a very large change in β_T and α over a short amount of time, about 200 hours (Figure 14). At longer times, the secondary structure no longer changed. Again, there was no change in the random coil fraction. Gd:My 1:1 produced a large amount of fibers approximately 10 μm in diameter and several hundred μm long.

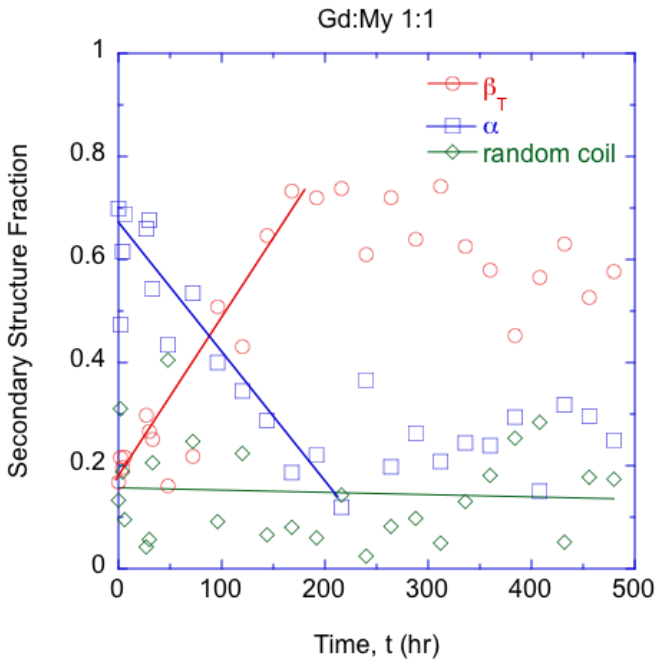

Figure 14 Secondary structure fractions for each of the secondary structures present within the Gd:My 1:1 system

Figure 14 shows the change in secondary structure. Figures 15-18 shows changes in the Amide I, Amide II, and Aliphatic regions.

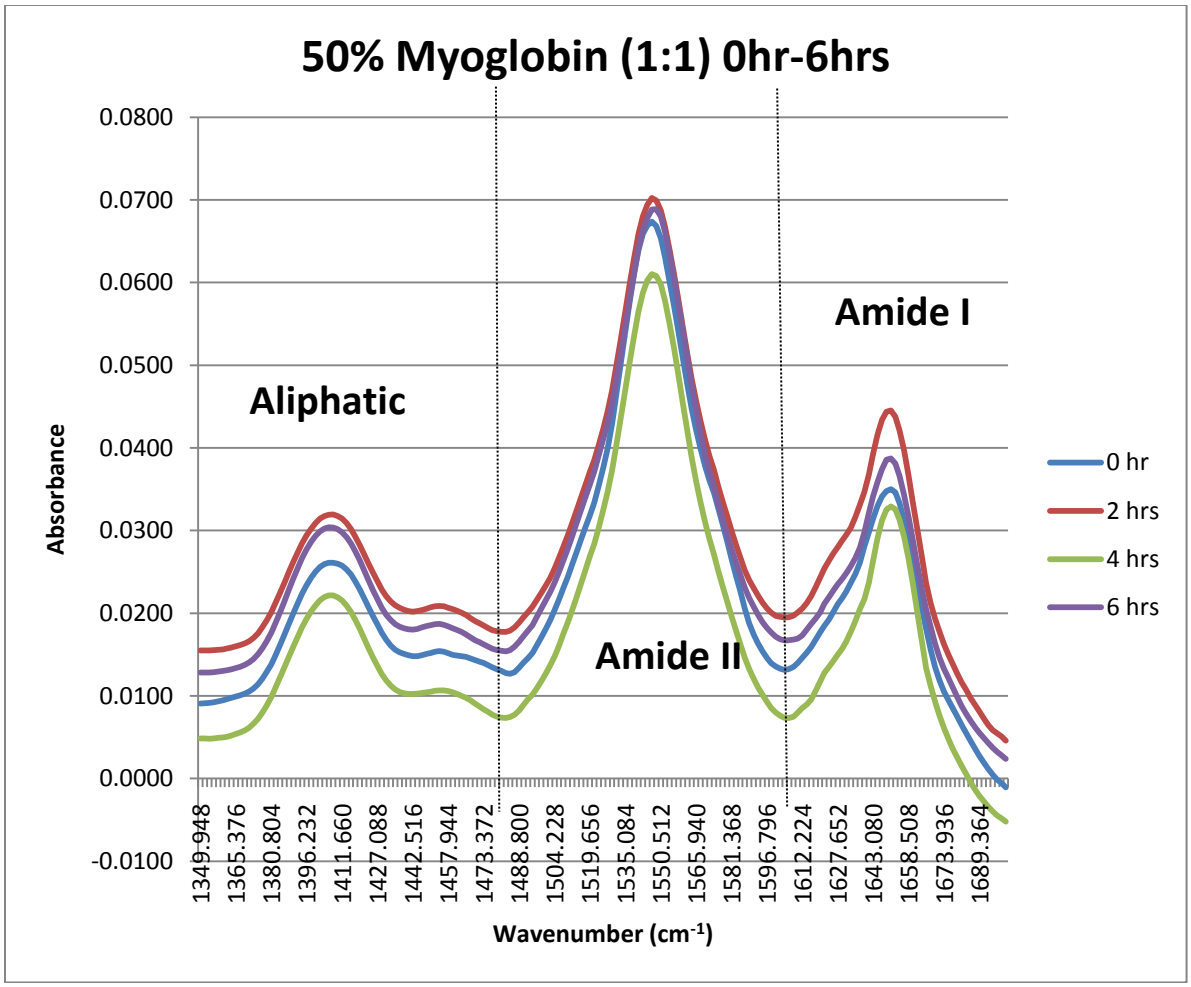

Figure 15 Gd:My 1:1 system during the first 6 hours

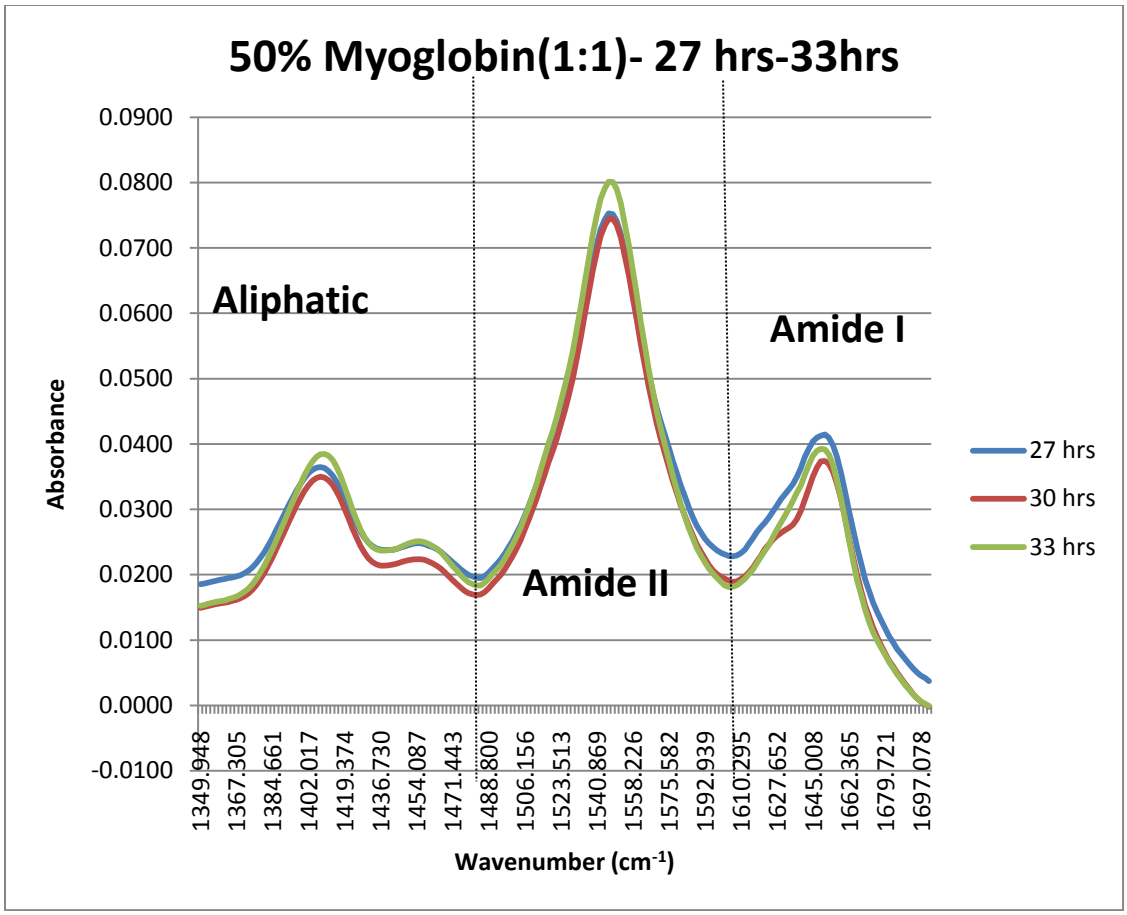

Figure 16 Gd:My 1:1 system shortly after 24 hours

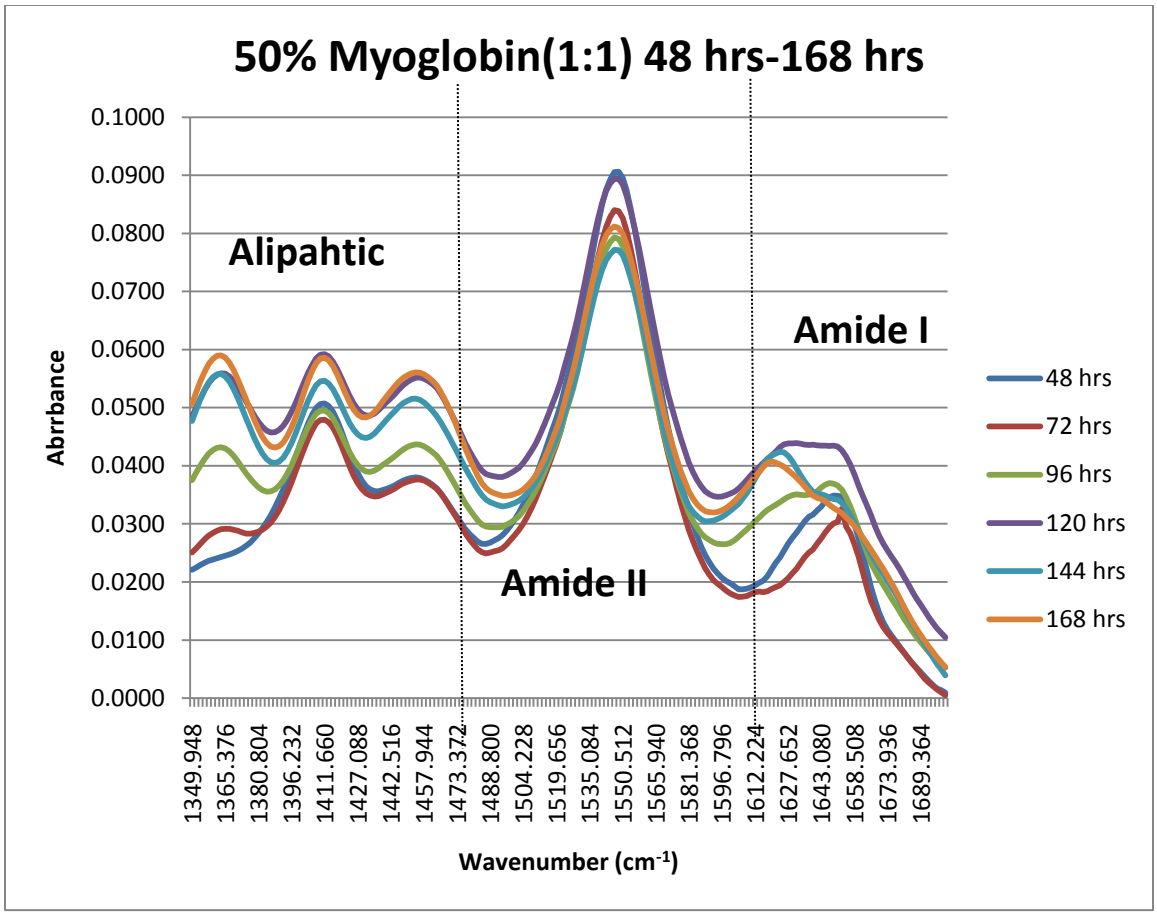

Figure 17 Gd:My 1:1 system during week 1

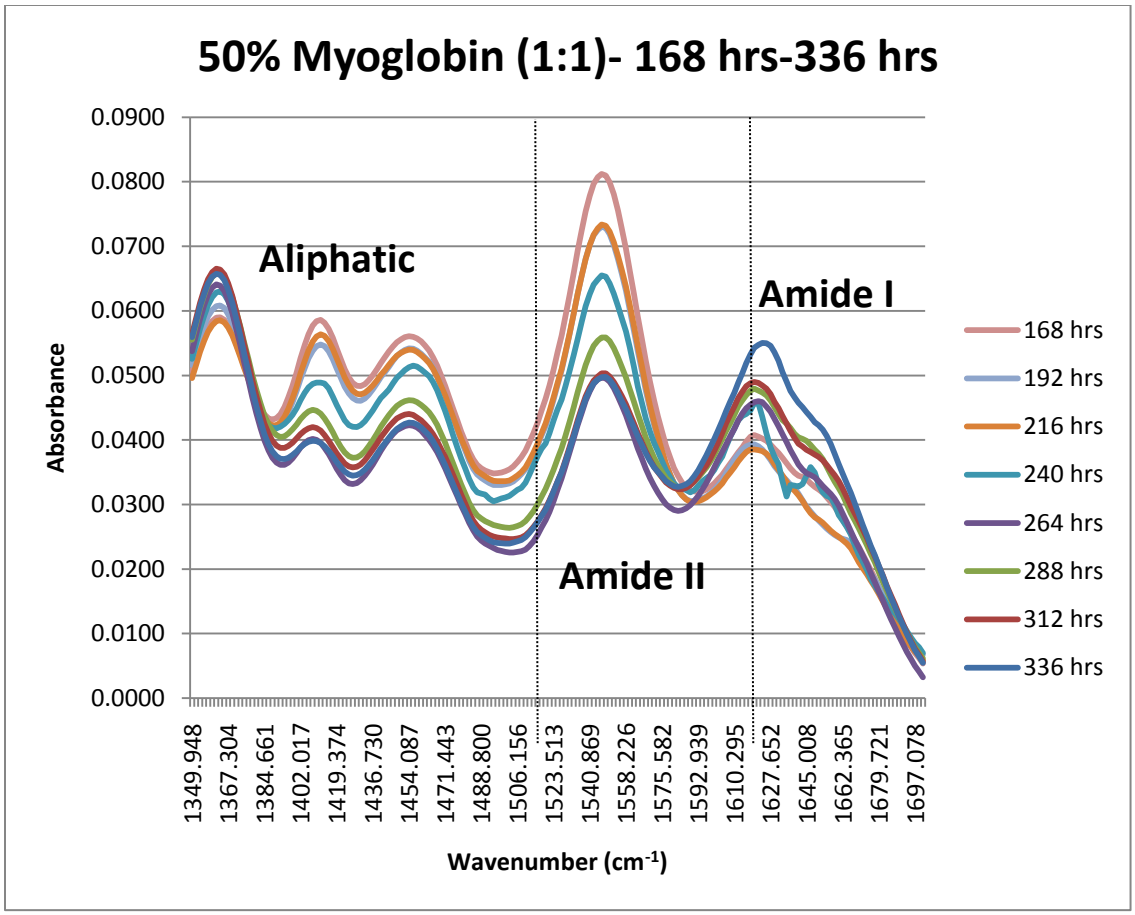

Figure 18 Gd:My 1:1 system during week 2

3.1.4 75% Gliadin and 25% Myoglobin (3:1)

Once Gd became the majority fraction, the overall change in β_T and α decreased again (Figure 19 for Gd:My 3:1) but did not change for all time like Gd:My 1:3, instead saturating at about 200 hours, which was similar to Gd:My 1:1. So the maximum change in secondary structure occurred for the equal mass fraction mixture. Gd:My 3:1 showed no change in random coil fraction and was a prolific fiber former.

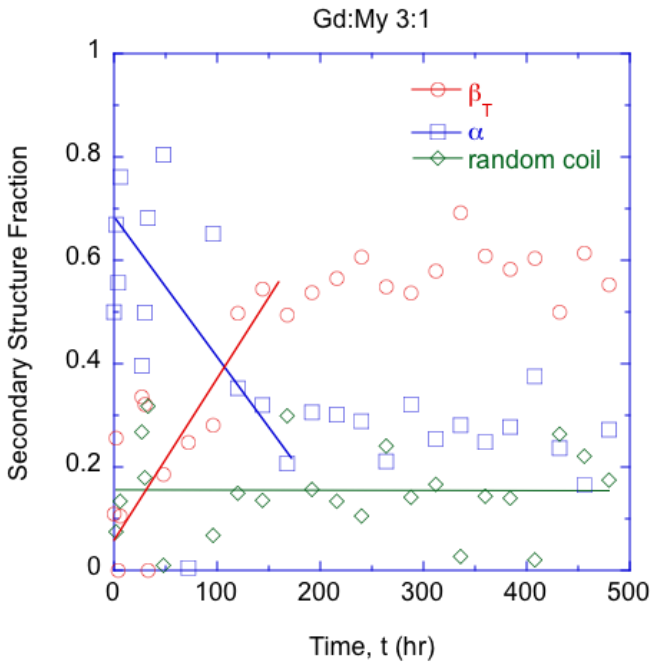

Figure 19 Secondary structure fractions for each of the secondary structures present within the Gd:My 3:1 system

For pure Gd, there was a change in β_T and α over all time and again no change in random coil (Figure 19). Figures 20-23 show the changes in the amide I, amide II, and aliphatic regions.

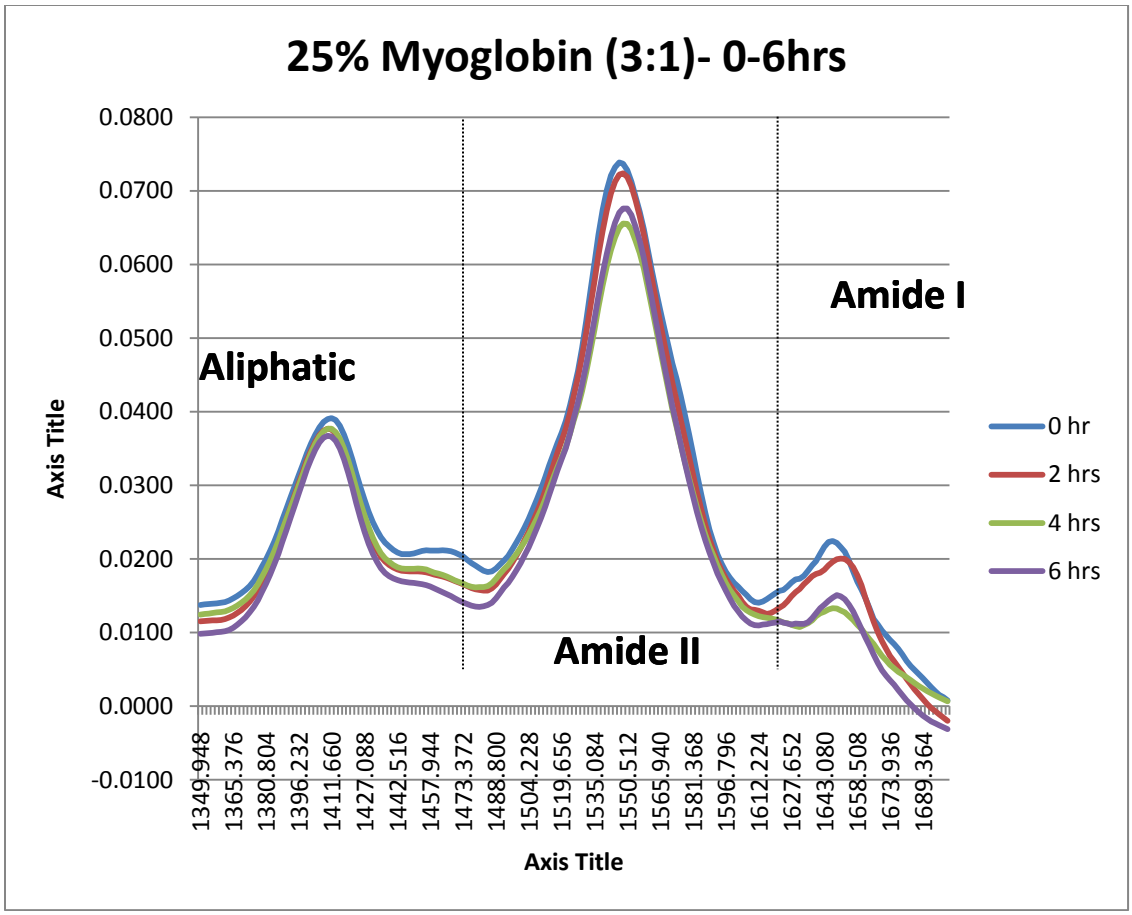

Figure 20 Gd;My 3:1 system during the first 6 hours

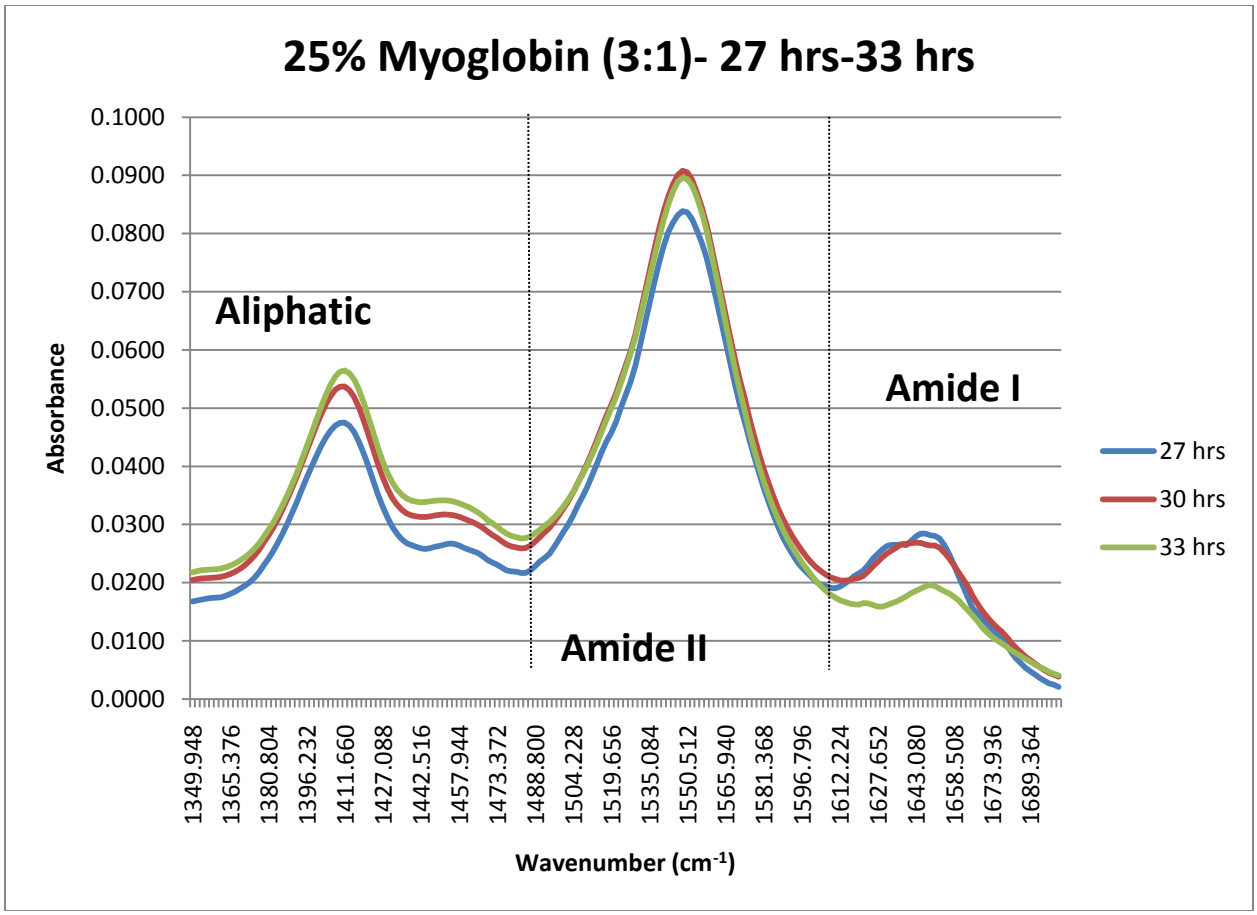

Figure 21 Gd:My 3:1 system shortly after 24 hours

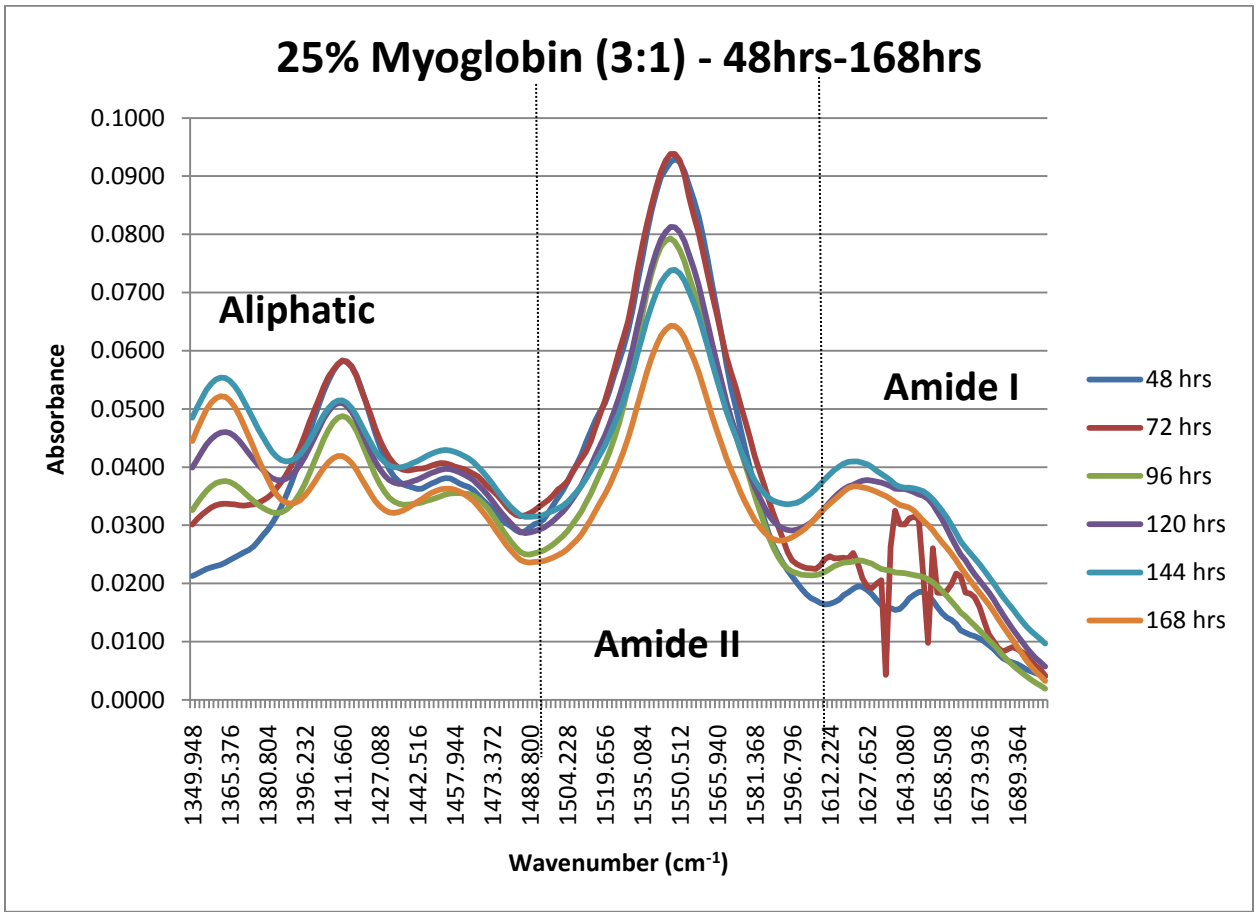

Figure 22 Gd: My 3:1 system during week 1

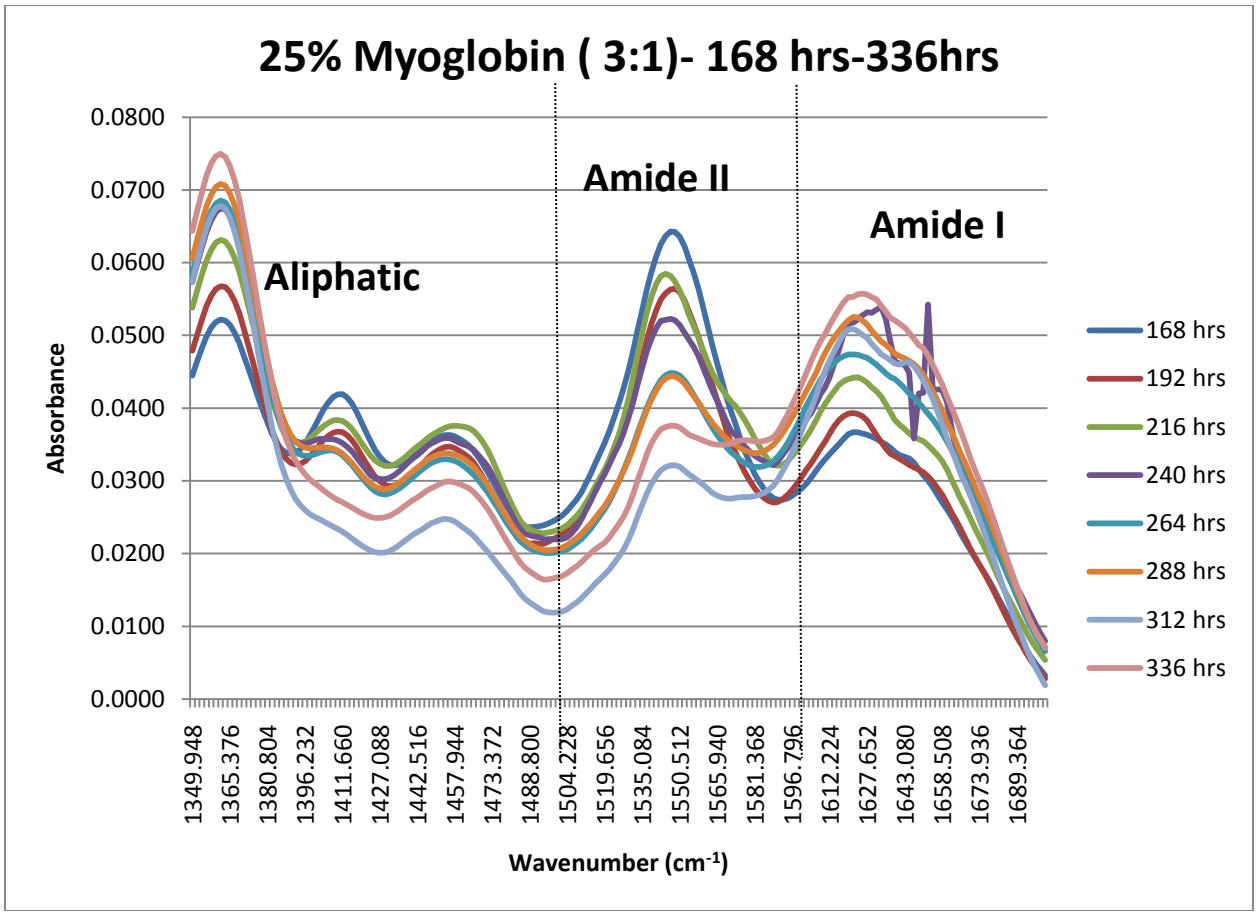

Figure 23 Gd:My 3:1 system during week 2

3.1.5 100% Gliadin and 0%% Myoglobin (1:0)

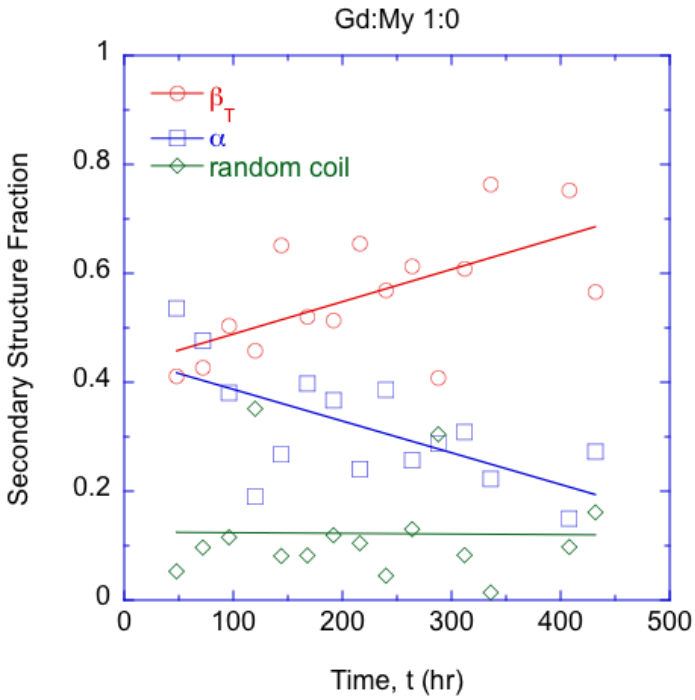

Figure 24 Secondary structure fractions for each of the secondary structures present within the Gd:My 1:0 system

Figure 24 shows the changes in secondary structure for the Gd:My 1:0 mixture. The changes in the Amide I, Amide II, and Aliphatic region are shown in Figures 25-28.

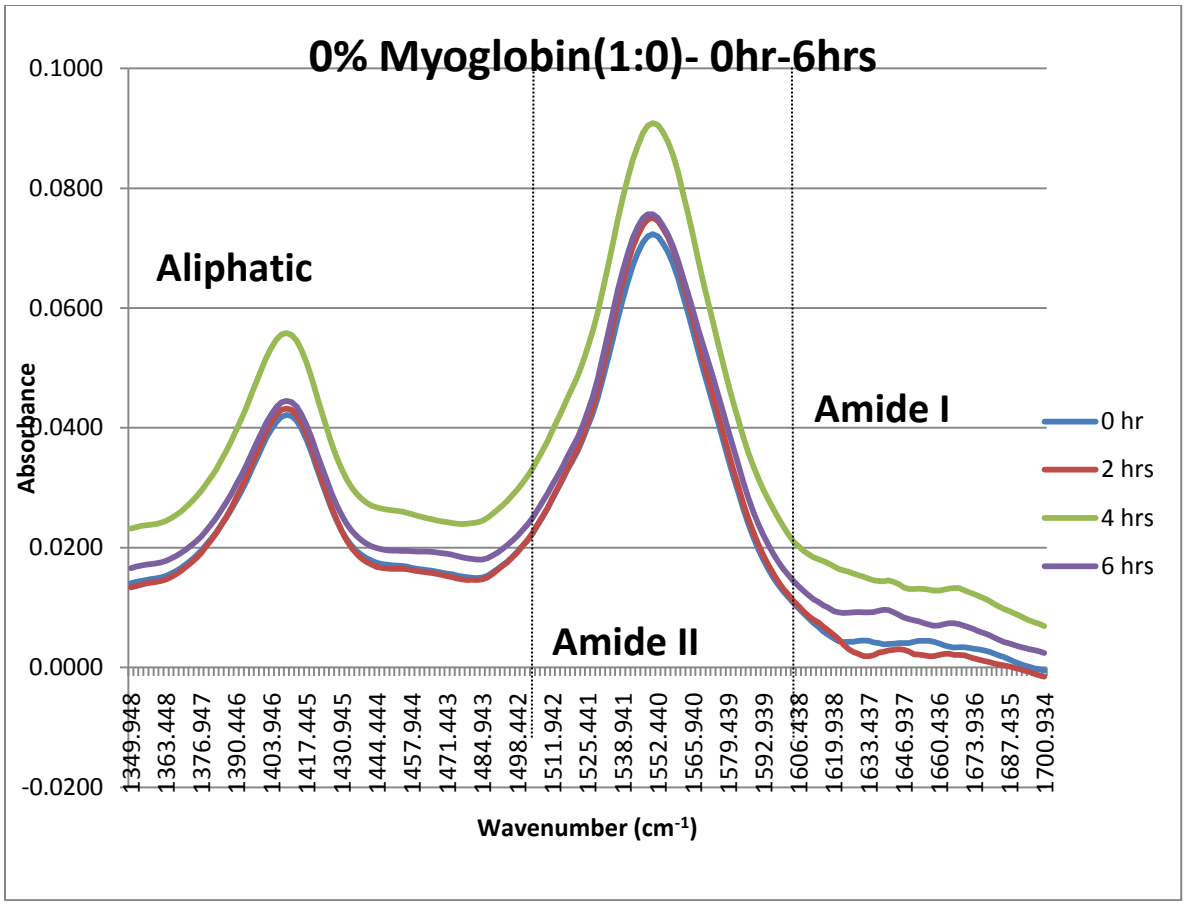

Figure 25 Gd:My 1:0 system during the first 6 hours

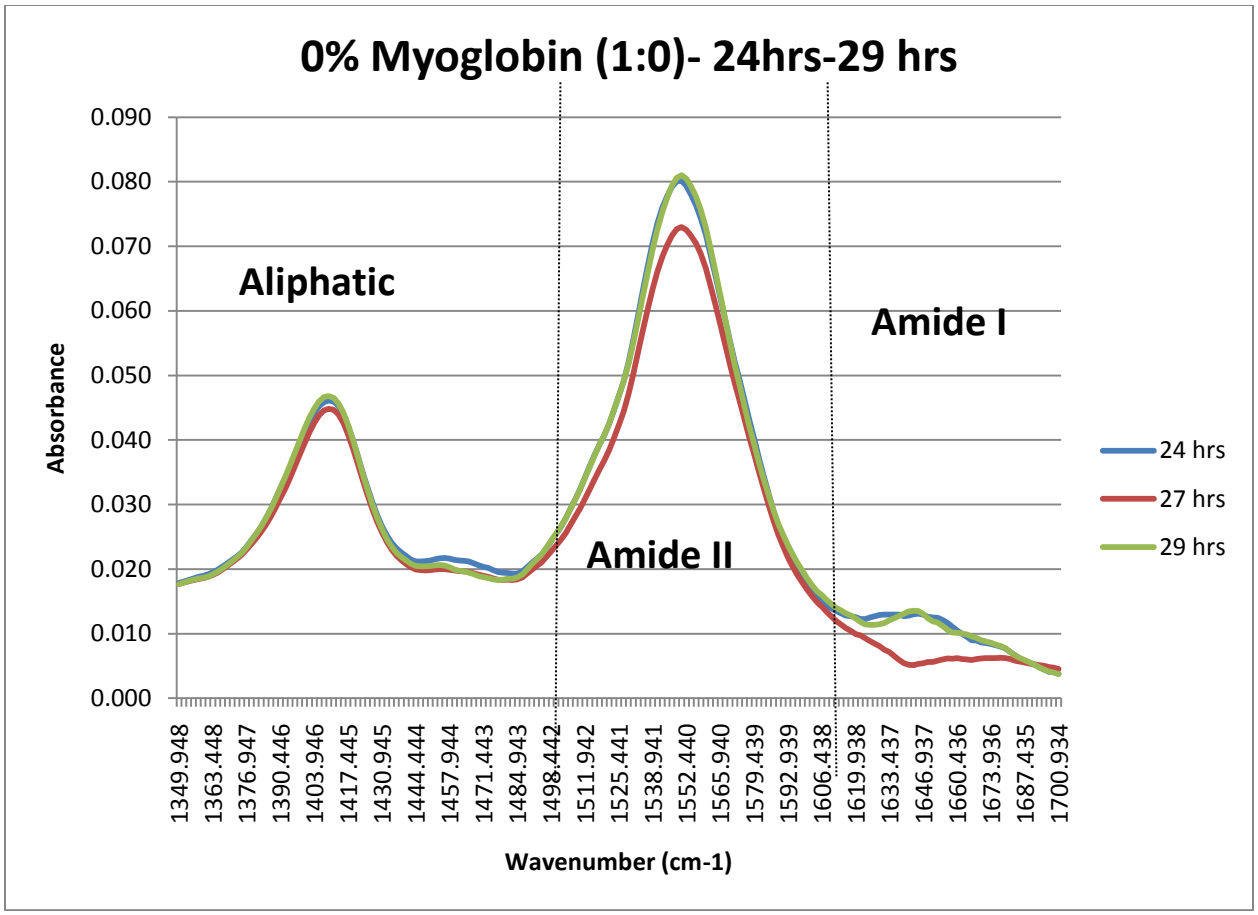

Figure 26 Gd:My 1:0 system within the first 24 hours

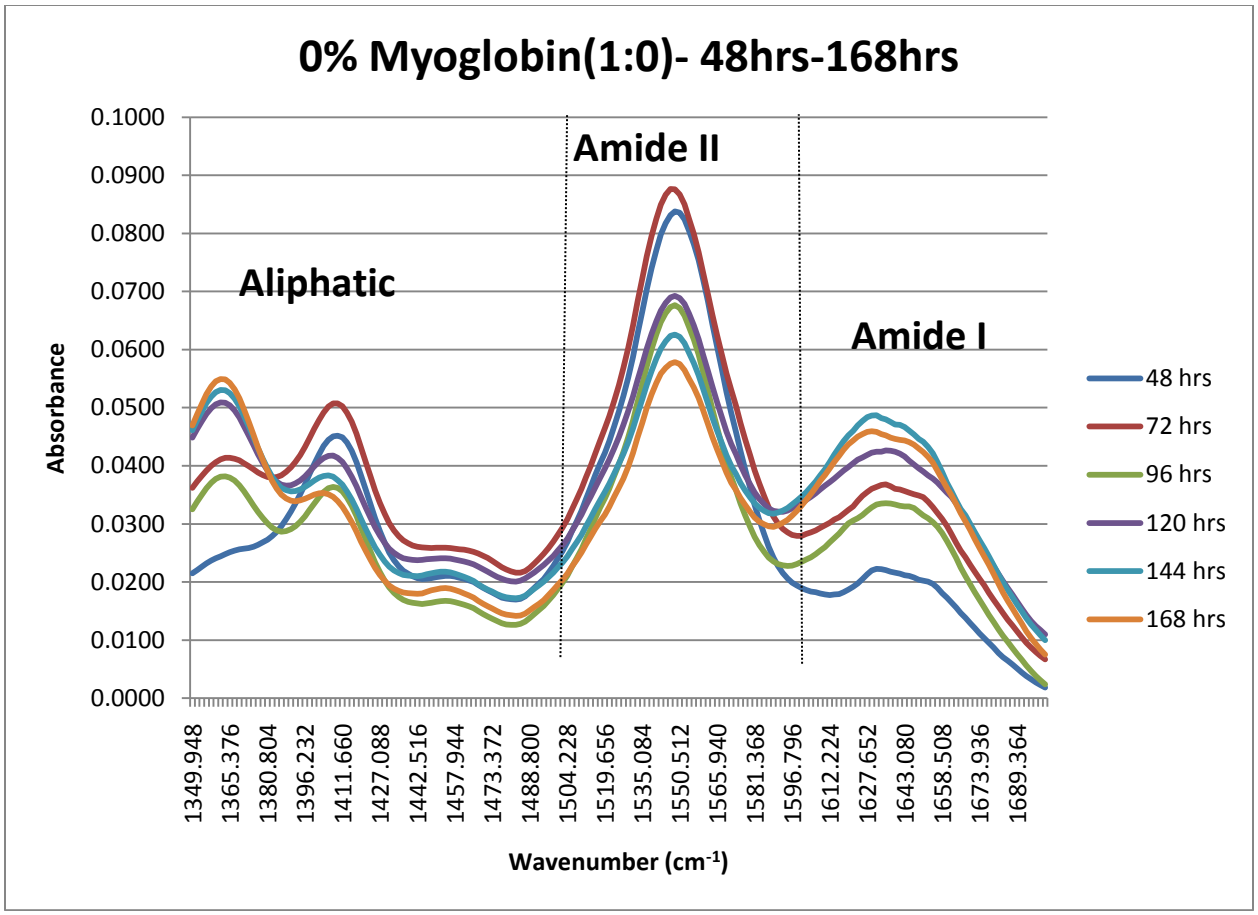

Figure 27 Gd:My 1:0 system during week 1

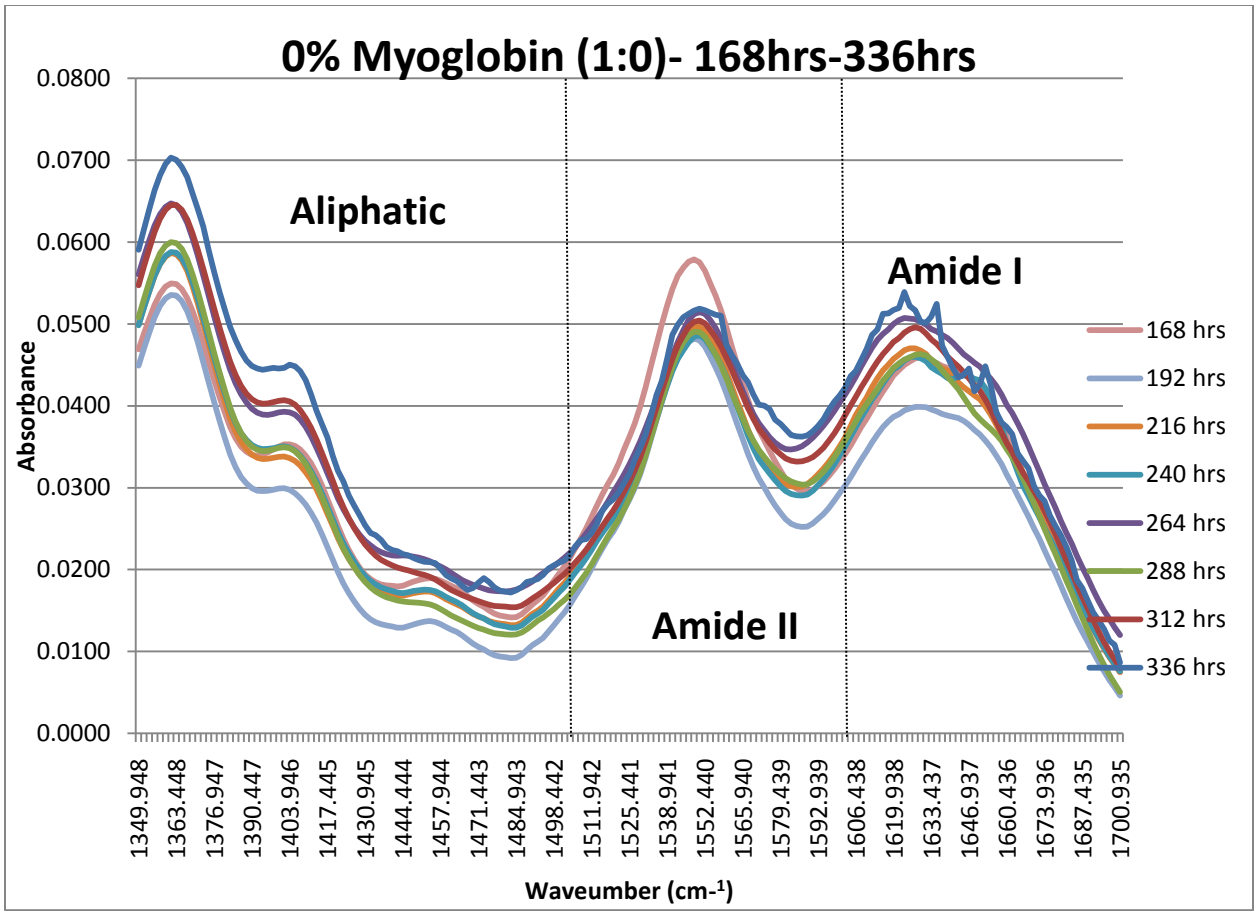

Figure 28 Gd:My 1:0 system during week 2

It was observed in the FT-IR spectra that severe changes occurred in the aliphatic region of each mixture and the pure proteins themselves. Specifically, the symmetric CH_3 deformation, $\delta_s(CH_3)$ at 1365 cm^{-1} increased and the asymmetric CH_3 deformation, $\delta_{as}(CH_3)$ at 1410 cm^{-1} decreased with time. Figure 29 plots the ratio $\delta_s(CH_3)/\delta_{as}(CH_3)$ for each sample as a function of time.

3.1.6 Symmetric and Asymmetric deformation

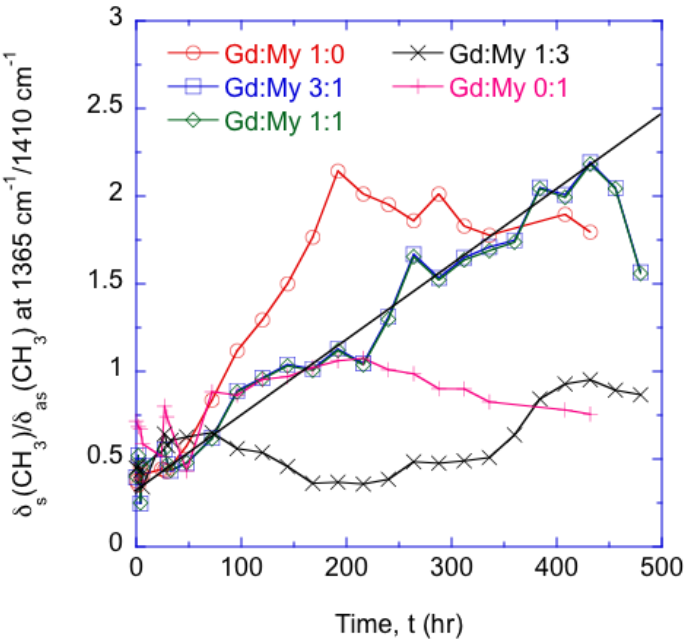

Figure 29 Ratios of symmetric and asymmetric deformation of CH_3

$\delta_s(CH_3)/\delta_{as}(CH_3)$ for Gd:My 3:1 and 1:1 continued to change for another 250 hours after β_T and α stopped changing. Gd:My 1:3 and 0:1 showed little change. Gd:My 1:0 displayed $\delta_s(CH_3)/\delta_{as}(CH_3)$ change until 200 hours and then it stopped but β_T and α continued to change.

Figure 30 shows that the solution pH during the experiment dropped then increased for all systems and the behavior was similar in each system.

3.1.7 pH Analysis of protein systems

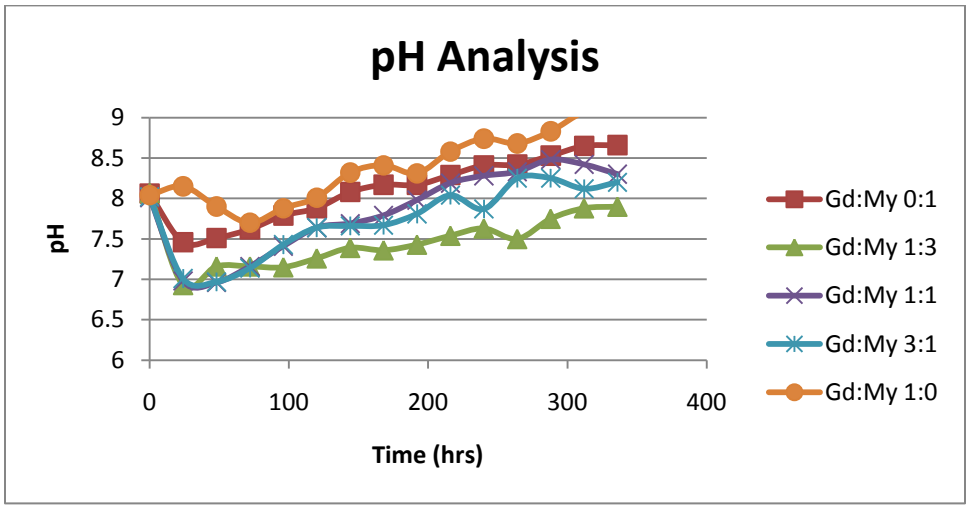

Figure 30 pH analysis of the protein systems

All of the peptide solutions showed the same pH behavior with time but much different chemical changes with time. Therefore, it appeared as if the pH changes were more dependent on deprotonation/protonation effects in water and not on peptide interactions so are not further considered in the self-assembly analysis.

3.2 Discussion

The results showed the following general phenomena:

1. A loss of α-helical structure with a concurrent gain in β-structures. The fraction of α-helix lost was approximately the fraction of β_T gained. All systems but pure myoglobin showed this behavior.
2. The loss of α-helix and gain in β_T occurred over different times for different systems. Gd:My 1:0 and 1:3 showed small but continuous change over all time

and did not form fibers. Gd:My 3:1 and 1:1 showed large but fast change in β_T and α, ending by about 200 hours. Gd:My 3:1 and 1:1 were very prolific fiber formers.

3. The ratio $\delta_s(CH_3)/\delta_{as}(CH_3)$ changed differently for different systems. There was little change over all time for Gd:My 1:3 and 0:1. Gd:My 1:0 showed a large change that saturated within 200 hours. Gd:My 3:1 and 1:1 showed a change until about 450 hours.

The results suggest a mechanism whereby elementary units or building blocks form first and then aggregate over much longer times into micron-sized fibers. Elementary units appeared to form from a loss of α-helix and gain of β-structures. Pure myoglobin showed no major change in β_T or α and no elementary unit or fiber formation. Pure Gd formed elementary units, which was consistent with the large amount of β-structures observed in XRD and FT-IR [1]. Pure Gd did not form large fibers. Gd:My 1:3 had elementary unit formation but limited large fiber formation. As shown in Figure 1(a), the fibers were short (0.1 mm at most) and not many were observed. Gd:My 3:1 and 1:1 showed elementary unit formation and a lot of large fibers. The fibers were consistently greater than 1 mm long. Therefore, there must be a criterion above and beyond elementary unit or cross-β formation that needed to be met to build large fibers. That requirement seemed to be the continued interaction of hydrophobic or aliphatic groups over long periods of time, i.e., for periods of time after elementary unit formation occurred. This was best exemplified by the changes in $\delta_s(CH_3)/\delta_{as}(CH_3)$. This ratio can be thought of as describing "packing" of CH_3 groups, which were plentiful in the hydrolyzed gliadin peptides as shown in Table 2. Amino acids alanine (A), valine (V),

leucine (L), and isoleucine (I) contain CH_3 in their side groups and are considered highly aliphatic. Threonine (T) contains CH_3 but is considered less aliphatic. $\delta_s(CH_3)$ measured the ability of the CH_3 groups to move up and down while $\delta_{as}(CH_3)$ measured the ability of the CH_3 groups to move side to side. As CH_3 groups packed tightly together, they lost the ability to move side to side in favor of up and down and the ratio increased. Looking back at the data, Gd:My 1:3 may not have had enough time to form fibers. The elementary unit formation was saturating at long times and the aliphatic packing was starting to increase at long times so the lack of fibers and the observation of short fibers may simply be a kinetic effect related to the lack of template.

Table 2 Tryptic peptides of gliadin (Uniprot P04721)

sequence	mol. wt. (kDa)	name	TANGO score
VPVPQLQPQNPSQQQPQEQVPLVQQQQFLGQQ QPFPPQQPYPQPQPFPSQQPYLQLQPFLQPQLPY SQPQPFRPQQPYPQPQPQYSQPQQPISQQQQQQ QQQQQQQQQQQQQIIQQILQQQLIPCMDVVLQ QHNIVHGK	16.4	Gd139	2
QQQQPSSQVSFQQPLQQYPLGQGSFRPSQQNP QAQGSVQPQQLPQFEEIR	5.7	Gd50	0
SQVLQQSTYQLLQELCCQHLWQIPEQSQCQAI HNVVHAIILHQQQK	5.4	Gd46	207
TFLILALLAIVATTATTAVR	2.1	Gd20	1477
NLARK	0.6	Gd5	0
MK	0.3	Gd2	0

TANGO is an algorithm that is used to predict the propensity of a given protein or peptide sequence to form cross-β structures at a given condition [2,3] . Also reported in Table 2 are the TANGO scores for the hydrolyzed gliadin sequences at the experimental conditions used in this study. Based on the TANGO analysis, the Gd20 and Gd46 peptides may be the ones most involved in the elementary unit and fiber formation process. Table 3 shows properties of Gd20 and Gd46 as well as GtL75, a tryptic peptide of low molecular weight glutenin, and myoglobin (My).

Table 3 Properties of proteins and peptides used in this study

Peptide	α(%)	# aa	MW	AI	GRAVY	pI	- (%)	+ (%)
Gd20	55	20	2060	171.0	1.820	9.4	0	5
Gd46	87	46	5422	108.0	-0.328	6.4	4.3	2.2
GtL75	68	75	8465	89.73	-0.668	5.4	2.7	1.3
My	74	154	17083	88.77	-0.381	7.2	13.6	13.6

α is % α-helix, # aa is number of amino acids, MW is molecular weight in g/mol, AI is aliphatic index, GRAVY is grand average of hydropathicity, pI is isoelectric point, and -, + is percentage of negative and positive amino acids, respectively.

Gd20, Gd46, and GtL75 were tryptic peptides of wheat gluten and the ones we hypothesized to be implicated in large fiber assembly because they had to be mixed together to produce fibers. They also had the highest TANGO scores. GtL75 had a TANGO score of 685 and was the only glutenin peptide with a predicted propensity for cross-β formation. Gd20 was the most aliphatic peptide with an aliphatic index of AI=171, which can be anticipated from its sequence because 18/20 amino acids contained

CH_3. Myoglobin was much less aliphatic, in fact it was polar, was neutral in charge, but was a much longer molecule with a lot of α-helix content. GtL75 and My had many traits in common. Myoglobin was a full peptide and shorter segments of it had TANGO scores from 64 to 348. So both had a theoretical propensity to form cross-β structures but not as high as Gd20. Experimentally, neither formed cross-β structures at the experimental conditions used in the TANGO prediction, suggesting that there was a threshold TANGO score for cross-β formation that was above 0, perhaps about 400 based on the limited results here. GtL75 and My were both polar while Gd20 was hydrophobic. GtL75 and My were both longer than Gd20 and higher in α-helix content. Based on the similarities in properties and the FT-IR observations with time, mixing myoglobin with hydrolyzed gliadin peptides supported our hypothesis that large fibers formed from mixtures of peptides with the right properties. Specifically, a short, hydrophobic "template" peptide will aggregate into cross-β structures and allow longer, hydrophilic "adder" peptides to undergo α to β transitions and add to the template. Both peptides need to have the ability to form cross-β structures at near physiological conditions. An elementary unit forms that at the right concentration of template to adder will continue to aggregate through hydrophobic packing of CH_3 on amino acid side groups into macroscopic fibers of well defined diameter and length.

Hydrolyzed gliadin showed some of these features but failed to produce large fibers. For instance, hydrolyzed gliadin showed elementary unit formation but only limited CH_3 hydrophobic packing. Gd46 had some of the characteristics of GtL75 and My but was slightly shorter and less hydrophilic. This suggested perhaps some critical length and

hydrophilicity of the “adder” peptide. Moving forward, we will separate the gliadin peptides and mix pure fractions of Gd20 and Gd46 to prove this.

3.3 References

[1] Ahmad I Athamneh and Justin,R.Barone, Enzyme-mediated self-assembly of highly ordered structures from disordered proteins, Smart Mater.Struct. 18 (2009) 104024.

[2] Tango 2011. http://tango.crg.es/.

[3] F Rousseau, J Schymkowitz, L Serrano. Protein aggregation and amyloidosis: confusion of the kinds? Curr.Opin.Struct.Biol. 16 (2006) 118-126.

[4] P Yu. Protein secondary structures (α-helix and β-sheet) at a cellular level and protein fractions in relation to rumen degradation behaviours of protein: a new approach. British Journal of Nutrition. 94 (2005) 655-665.

[5] H Susi, DM Byler. Fourier Deconvolution of the Amide I Raman Band of Proteins as Related to Conformation, Applied Spectroscopy. 42 (1988) 819-826.

Chapter 4: Conclusion

4.1 Conclusion

We have discovered a very unique combination of peptides that self-assemble into micron-sized fibers at physiological conditions. This sort of assembly beyond the nanometer scale is very unusual. The peptides are an α-helix containing "adding" peptide or protein and a β-sheet containing "templating" peptide or protein. At near physiological conditions (37˚C and pH=8) we can induce an α to β transformation in one or both of the peptides. It is not clear if the template must contain α-helices as well and further work must be done to confirm this. The smaller peptide is the template and larger peptides are the adders and again this condition must be further validated.

Aggregation began first with the 3:1 system because of the dominance of beta sheet templates (75% gliadin). This abundance assisted the alpha to beta transition because the alpha helix had room to insert into the template. Once the helix content was fully unraveled and inserted, aggregation ceased because of the lesser amount of myoglobin. The similar case was noticed for the 1:3 system but there was less template so the unraveled alpha helices had no place to insert once the template was fully filled. The 1:1 system had the largest changes in spectral regions, pH and beta secondary structure percent. The energy barrier of alpha helix and beta sheet vary largely and increases the difficulty of monitoring the transition. We have shown that monitoring the transition is possible with ATR FT-IR.